

Wildfire Controls on Evapotranspiration in California's Sierra Nevada

Qin Ma^{a,b}, Roger C. Bales^{a,c}, Joseph Rungee^{a,c}, Martha H. Conklin^{a,c}, Brandon M. Collins^{d,e}, Michael L. Goulden^f

^aSierra Nevada Research Institute, University of California, Merced. ^bDepartment of Forestry, Mississippi State University, MS. ^cSchool of Engineering and Environmental Systems Graduate Group, University of California, Merced. ^dUSDA Forest Service, Pacific Southwest Research Station, Davis, CA. ^eCenter for Fire Research and Outreach, University of California, Berkeley. ^fDepartment of Earth System Science, University of California, Irvine.

Highlights

- On average, evapotranspiration dropped 265 mm yr⁻¹ during the 1st year after a fire, and 169 mm yr⁻¹ over 15 years.
- Wildfire impacts on evapotranspiration were greatest in dense, mid-elevation (900-1300 m asl) forests.
- Restoration of forest density to near historical conditions, or an equivalent increase in wildfire, could further reduce evapotranspiration by up to 9%.

Abstract

We used Landsat-based measures of annual evapotranspiration (ET) to explore the effects of wildfires on vegetation water use across California's Sierra Nevada. Wildfires decreased ET relative to unburned and pre-fire controls, in many areas this reduction persisted for at least 15 years. The ET reduction averaged 265 mm yr⁻¹ (36% of pre-fire ET) during the first year after fire, and 169 mm yr⁻¹ (23%) over the first 15 years after fire. The ET reduction varied with burn severity, pre-fire canopy density, and hydro-topographic environment. In areas burned at low severity the ET reduction in the first year after fire averaged 224 mm yr⁻¹ (31% of pre-fire ET) whereas high severity were reduced a 362 mm yr⁻¹ (50%) for the first year. Forest stands that were denser pre-fire had a larger ET reduction across all burn severities. Evapotranspiration reduction following moderate-to-high-severity burns was greatest at 900-1300 m asl elevation. The combination of pre-fire canopy density and burn severity explained 70% of the spatial variation in first-year ET reduction. Forest restoration and a reintroduction of low-intensity fire have been proposed as management practices to mitigate fire risk and improve ecosystem health. Our findings illustrate that restoration and fire reintroduction may reduce the current total ET by up to 9%, with potential benefits for downstream water supply in a globally important food-producing region.

1. Introduction

Many Western United States forests are severely overstocked with high densities of small trees owing to fire suppression and logging of large trees since the early 20th century (Collins et al. 2017a; Hessburg et al. 2005; Knapp et al. 2013; Miller et al. 2012; Safford and Stevens 2017). These forest management practices have also led to the accumulation of ladder and surface fuels, which coincide with climate warming, has contributed to progressively larger and more-severe wildfires (Collins et al. 2017a; Westerling et al. 2006). Mitigating the wildfire hazard in these highly altered forests by reducing tree density and fuel loads will also change the water balance; and these potential water co-benefits should be considered in designing and evaluating restoration treatments (Roche et al. 2020; Saksu et al. 2020). Uncharacteristically dense forests have not only reduced overall water yield but also increased inter-tree competition for water, making contemporary forests more vulnerable to drought and insect attack (Bales et al. 2018; Goulden and Bales 2019; Liu et al. 2019; Stephens et al. 2018; Young et al. 2017). While monetizing water-related benefits of thinning has the potential to help offset costs, lack of regionally relevant data to project and

verify these benefits is a barrier to comprehensively planning and evaluating forest-thinning projects.

Mechanical thinning, prescribed fire, and managed wildfire can mitigate the risk of high-severity wildfire, while reducing evapotranspiration (ET) and plant stress, and also increasing water yield (Andréassian 2004; Battles et al. 2018; Boisramé et al. 2017; Boisramé et al. 2018; Boisramé et al. 2019; Hallema et al. 2018b; Hibbert 1965; Knapp et al. 2017; Saksu et al. 2017). However, the effect of fire on ET is highly variable, depending on pre-disturbance vegetation composition and condition, climate, topography, disturbance severity and recovery rate (Bart et al. 2016; Nolan et al. 2014a; Nolan et al. 2015; Nolan et al. 2014b; Poon and Kinoshita 2018a; Wittenberg et al. 2007).

Past studies provide a limited basis for predicting how forest-water-use patterns across a specific region change with disturbance. Whitehead and Kelliher (1991) modeled water use in a conifer forest and found that a 42% reduction in leaf area index (LAI) resulted in 36% less annual canopy transpiration, and 27% less canopy evaporation. Saksu et al. (2017) found that light thinning (8% reduction in LAI)

increased mean-annual runoff by 14% in a high-precipitation central-Sierra catchment, but had less noticeable impact in a low-precipitation Southern Sierra location. They suggested that this lack of hydrologic impact in the drier site was due to vegetation regrowth that offset the effect of thinning and/or precipitation variability masked the effects. Likewise, Bart (2016) found that the response of runoff to disturbance is often obscured by high interannual precipitation variability. Assessments of the effect of fire on the water balance based on annual river flow suggest that moderate-to-high severity wildfire enhances discharge for five years or longer (Hallema et al. 2018a; Hallema et al. 2018b; Hallema et al. 2017); however, precipitation variability introduces considerable uncertainty in these analyses.

Recent advances in estimating evapotranspiration with remote sensing provide a more-direct strategy to quantify changes in vegetation water use following disturbance. Evapotranspiration can be estimated using bottom-up physically based models (Jin et al. 2011; Ryu et al. 2011), or top-down data-driven methods based on remote-sensing imagery and extrapolated meteorology (Li et al. 2018; Poon and Kinoshita 2018a; Xiao et al. 2008). Goulden et al. (2012) developed a simple, data-driven method for distributing eddy-covariance ET measurements from individual sites using a relationship with satellite observations of Normalized Difference Vegetation Index (NDVI). This method has been successfully used to map ET in Sierra Nevada forests (Goulden et al. 2012; Goulden and Bales 2014; Roche et al. 2018). Roche et al. (2018) subsequently used this approach to explore the effects of management and fire on evapotranspiration on several patches of Sierra Nevada forest. These previous studies demonstrated the effectiveness of using data-driven approach to quantify evapotranspiration changes over the Sierra Nevada forests.

Our goal was to broaden the investigation of wildfire impacts on vegetation water use by analyzing wildfires during 1985-2017 throughout the Sierra Nevada and southern Cascade Range. We created and used an annual, 30-m resolution evapotranspiration dataset to explore the changes in vegetation water use before and after large wildfires. We focused on three questions: First, how much does wildfire affect evapotranspiration, and how have the effects of wildfire on Sierra Nevada evapotranspiration varied over the past three decades? Second, how

does the effect of wildfire on evapotranspiration vary with fire severity, pre-fire vegetation condition, climate, and landscape attributes? Third, how would a future increase in fire occurrence across the Sierra Nevada affect evapotranspiration?

2. Data and methods

2.1 Study area and fires. We considered most of the large wildfires that occurred in the Sierra Nevada and Shasta river basin from 1985 to 2017 (Fig. 1). The study area covered 137,037 km² and contained 14 major source-water basins that provide over 60% of California's water supply (Bales et al. 2011; Bales et al. 2006). Sierra Nevada forests are home to diverse conifer species, contain large carbon stocks, and provide important wildlife habitat (North 2012). The study area has complex terrain, with steep elevation and climate gradients, and large inter-annual precipitation variability (Bales et al. 2006).

California's climate is Mediterranean, with cool-wet winters followed by warm-dry summers, which creates conditions conducive to wildfire. The annual area burned and fire severity have increased in recent decades due to fuel accumulation and longer fire seasons (Westerling et al. 2006).

We used fire records from the "Vegetation Burn severity classified by change in Basal Area" dataset (<https://www.fs.usda.gov/detail/r5/landmanagement/gis/?cid=stelprd3804878>, accessed Jan 2020), which includes fire perimeter, timing, and burn severity for 635 large fires (>4 km²) in California based on Landsat imagery. Burn severity was broken into six classes based on basal-area loss (0-10, 10-25, 25-50, 50-75, 75-90, and 90-100%). The Relative Differenced Normalized Burn Ratio (RdNBR) (Miller and Thode 2007), calculated from the pre- to post-fire change in Landsat imagery, was used to classify burn severity by reference to the field-measured Composite Burn Index (Miller et al. 2009; Miller and Quayle 2015). The burn severity is a relative measure based on the normalization of each image, and thus was only used as an indicator of relative fire-severity class rather than the exact amount of basal area reduction. The fire-severity dataset had a 30-m resolution, which we resampled into 200-m pixels using the majority method. This coarser resolution reduced noise from the fire-severity classification and also computational load. The analysis ultimately

considered approximately 300,000 pixels during 1985-2018.

2.2 Analyzing evapotranspiration responses to fires. Gridded annual ET from 1985 to 2018 was calculated using a non-linear, data-driven regression method based on the correlation between eddy-covariance measurements of annual evapotranspiration and satellite imagery derived NDVI, updated through 2016 (Goulden et al. 2012). The ET data can be downloaded from <https://doi.org/10.6071/M3010D>. More information about ET estimation is included in the supplementary material “ET estimation method” and Fig. 1 and S1 (Goulden et al. 2012; Goulden and Bales 2019; Su et al. 2017; Sulla-Menashe et al. 2016). From gridded data we derived both the absolute (aET) and relative (rET) reduction in evapotranspiration caused by fire:

$$aET_i = (ET_{i-1} - ET_i) - (ET_{i-1}^{nofire} - ET_i^{nofire}) \quad (1)$$

$$rET_i = 100\% \times aET_i / ET_{i-1} \quad (2)$$

where aET_i and rET_i are the absolute and relative ET changes in year i .

ET_{i-1} and ET_i indicate the ET value in burned areas estimated one year before the fire and in year i , respectively. ET_{i-1}^{nofire} and ET_i^{nofire} indicate evapotranspiration in unburned control areas estimated one year before the fire and in year i , respectively.

The unburned areas were used as a control, or reference, to isolate the change in evapotranspiration caused by fire alone. The unburned control pixels were selected for each fire using two criteria. First, unburned controls were outside the 10-km buffer zone of a fire perimeter, but within the same 12-digit hydrologic unit code watershed (<https://water.usgs.gov/GIS/huc.html>), as areas in the same watershed were viewed as more likely to be hydrologically similar. Second, unburned controls were located within the same 100-m elevation bin as burned pixels.

We explored the correlations between fire-caused changes in aET and rET , and eleven attributes from three categories (Table 1): i) Pre-fire vegetation condition, represented by five-year-average pre-fire NDVI and pre-fire vegetation types from National Land Cover Database (NLCD in 1992, 2001, 2006, and 2011), ii) landscape and climate, i.e. elevation, slope, Northness (combined slope and aspect), latitude, and daily temperature and annual precipitation averaged over 1985-2018, iii) fire

characteristics, represented by fire size, change in Normalized Burn Ratio (dNBR), and Relative differenced Normalized Burn Ratio (RdNBR).

We further analyzed the relationship between the evapotranspiration change with fire of each severity and four sets of possible correlates: i) pre-fire NDVI (five-year-average), ii) local climate (average precipitation and temperature over 1985-2018), iii) elevation, and iv) fire severity (Table 1). The mean effects of fire on evapotranspiration were calculated for 100-mm wide precipitation bins, 0.1 NDVI unit bins, 1°C temperature bins, 100-m elevation bins for three fire-severity classes, i.e. 0-25%, 25-75%, and 75-100% basal arear reduction. The samples size in each bin varied from 100 (bins with fewer than 100 pixels were excluded) to 50,000 pixels, which represent areas of 4 km² to 2000 km².

2.3 Predicting evapotranspiration reduction.

We applied two statistical methods to further explore the effects of fire on evapotranspiration: multi-variable linear (Fig. S2) and random-forest regression (Fig. S3) (Breiman 2001). Both methods have been applied to similar problems. Ma et al. (2017) used the multi-variate linear regression to model individual tree growth in Sierra Nevada forests; and Boisramé et al. (2018) used the random-forest to illustrate how vegetation, fire history, and landscape positions influenced water availability in a restored Sierra Nevada forest. Both models were trained using a randomly selected subset of 10% of the burned pixels, and prediction accuracy was evaluated by comparison against the remaining 90%. These training and testing processes were repeated 10 times, and model skill assessed by R² and RMSE averaged across the runs.

We also projected the possible Sierra-wide reduction in aET under three possible disturbance scenarios. First was a <25% basal-area reduction, equivalent to low-severity fire, as might occur with a widespread reintroduction of low-intensity prescribed fire and light mechanical thinning to reduce surface fuel (Saksa et al. 2017). Second was a 25-75% basal-area reduction, as might occur with a systematic effort to restore historic conditions using thinning, prescribed fire, and managed wildfire. Moderate-severity fires in fire-excluded forests provide a biomass reduction that approximates the structure reported for early 20th century forests (Collins et al. 2011; Collins et al. 2017a; Collins et al. 2018). Third, we considered

widespread severe fires resulting in >75% basal-area reduction, as might occur with frequent severe fires in the absence of efforts to decrease fuels.

We used Landsat-derived indices of fire severity and vegetation conditions to model the possible ET reduction with fire. We summarized the mean and standard deviation values of the fire index (dNBR) over areas burned during 1985-2017 to indicate fire-severity classes (Fig. S4b). Forest density was represented by the current NDVI and vegetation type map, for which only dense forests (annual mean NDVI>0.4 during 2018 and forest land cover types in NLCD2016) in the 500-2500 m elevation range were included. An additional restriction for this analysis was that forests had not been burned in a large wildfire in the past 20 years (Fig. S4), given the expectation that these locations will have higher fuel loads and fire risks, and will be a higher priority for restoration. The evapotranspiration reductions from altered fire frequencies and severities were modelled based on the dNBR ranges and NDVI map over 15 years following fire (Fig. S5). The 15-year total evapotranspiration reduction was estimated as a ratio compared to the 1st year post-fire ET reductions (Fig. 3; Table S1).

3. Results

3.1 Fire pattern and evapotranspiration disturbance

The area burned annually averaged 244 km² yr⁻¹ during 1986-2000 period and increased to 457 km² yr⁻¹ for 2001-2017 period (Fig. 2). The 1st year post-fire ET reduction across the area ranged from 4×10⁻³ billion m³ yr⁻¹ in 1995 to 0.3 billion m³ yr⁻¹ in 2015 (Fig. 2a). The local mean evapotranspiration reduction, calculated as the total evapotranspiration change divided by the total burned area, averaged 265±79 mm yr⁻¹ (mean±std, calculated from Equation 1). Both annual area burned and evapotranspiration reduction were correlated with mean annual temperature, with a Pearson's r of 0.54 and 0.51, respectively (p value<0.01).

Aggregating across all fires shows a consistent pattern of ET reduction in the first year after fire, followed by a gradual recovery over the subsequent 15 years (Fig. 3a). The ET reduction relative to the pre-fire and unburned control values in the first year after fire averaged 224 mm yr⁻¹ in the lowest fire severity class (<10% basal area mortality) and 362 mm yr⁻¹ in the highest fire severity class (>90% basal area

mortality) (Fig. 3b). The ET recovery in all burn classes had not completely recovered after 15 years, and the mean ET across low burn severity pixels was still only ~80% of that in the unburned controls. This lack of complete recovery across the population of low burn severity pixels reflected spatial heterogeneity in recovery rate. More than 65% of these pixels ET had recovered fully by 15 years, while the remaining ~35% still had reduced ET relative to the unburned control (Fig. 3c). The mean rate of ET recovery in each burn class began to level off over time (Fig. 3b). ET varied little over the five years before fire, with slightly lower values for areas that burned with moderate-to-high severity (>25% basal area mortality) (Fig. 3a).

3.2 Attributes correlated with

evapotranspiration response. The correlation matrix (Fig. 4) showed that first-year post-fire ET reduction (aET) was most-strongly correlated with the five-year average pre-fire NDVI (bNDVI, r = 0.74), followed by dNBR (r = 0.66) and precipitation (r = 0.47). The linear relationships of environmental attributes with relative ET reduction (rET) were less strong than those with aET. dNBR showed positive correlations with rET reduction (r = 0.65). There were additional correlations among the Landsat-derived indices (bNDVI, dNBR, RdNBR), between bNDVI and precipitation, elevation and temperature, and between aspect and slope. Some non-linear relationships were observed between the ET reductions and environmental attributes (Fig. S3).

Both *rET* and *aET* were greater in areas with denser pre-fire vegetation (bNDVI; Fig 5). The fire-impacted areas were evenly distributed across bNDVI values of 0.3-0.7 (Fig. 5a). For areas burned at moderate-severity (25-75% basal area reduction) *rET* exceeded 35% and *aET* exceeded 200 mm yr⁻¹ for areas with bNDVI higher than 0.5 (Fig. 5b and 5c). For NDVI between 0.5-0.7, each 25% reduction in basal area resulted in a 30-80 mm yr⁻¹ drop in ET.

Most fire-impacted areas had a long-term mean precipitation of 200-900 mm yr⁻¹, with *aET* and *rET* significantly larger in wetter areas (800-1500 mm yr⁻¹) (Fig. 5d, 5e, 5f), coincident with higher rates of evapotranspiration (>700 mm yr⁻¹) in the unburned controls. Areas burned at moderate-severity *aET* was 300-400 mm yr⁻¹, with *rET* being 40-60% for higher-precipitation areas (Fig. 5e, 5f).

Evapotranspiration in unburned areas peaked ($\sim 750 \text{ mm yr}^{-1}$) at 600-1200 m elevation, whereas fires occurred over a wider elevation range, with extensive burning at 500-2000 m (Fig. 6a). The aET peaked at mid-elevation (900-1300 m), with a smaller aET at lower and higher elevation (Fig. 6b). The aET reached 400 mm for high-severity areas (75-100% basal-area reduction) at mid-elevation (900-1300 m), with a moderately lower aET in less-severe burns (Fig. 6b). The rET range was 40-60% for most moderate-to-high severity burns (Fig. 6c). The majority of fires occurred in areas with a mean temperature of 7-16°C (Fig. 6d). Pre-fire evapotranspiration was greatest ($>650 \text{ mm yr}^{-1}$) at a mean temperature of 12-15°C. The absolute reduction in ET was greatest at a mean temperature of 11-14°C (Fig. 6e). The rET was higher in cooler zones (Fig. 6f). The ET trends with temperature broadly paralleled those with elevation (Fig. 6), reflecting the negative correlation between temperature and elevation (Fig. 4).

3.3 Prediction of possible ET reduction with changes in fire. The multivariate-linear-regression model (Equation 4) that combines $dNBR$ and five-year-average pre-fire NDVI ($bNDVI$) achieved a R^2 of 0.70 and RMSE of 105 mm in modeling aET .

$$aET = 0.41dNBR + 622.84bNDVI - 234.61 \quad (3)$$

The addition of further variables into the model only improved the overall accuracy marginally (R^2 from 0.7 to 0.73, Fig. S2).

The random-forest regression achieved a higher accuracy in modeling aET , with an R^2 of 0.81 and RMSE of 83 mm. The random-forest regression also showed $bNDVI$ and $dNBR$ to be the most-important variables. Nine additional variables contributed to the improvement of the random-forest model fit for aET (Fig. S3), but with an increased risk of over-fitting and collinearity.

We used the multivariate-linear-regression model (Equation 4) to estimate how potential change in ET was influenced by fire severity in dense, long unburned forests. Our forest area analyzed accounted for 27% (37,000 km^2) of the total Sierra Nevada (137,037 km^2) and 68% of the forest area (54,412 km^2). The resulting Sierra Nevada-wide evapotranspiration reduction in the 15-year post-treatment period was 5.3 ± 1.0 billion $\text{m}^3 \text{ yr}^{-1}$ (mean \pm sd) for areas burned at moderate severity, equivalent to $9 \pm 1\%$ of the current

annual evapotranspiration. The evapotranspiration reduction was 4.4 ± 0.9 billion $\text{m}^3 \text{ yr}^{-1}$ for areas burned at low-severity, and 6.5 ± 1.3 billion $\text{m}^3 \text{ yr}^{-1}$ for high severity areas (Fig. S5, Table S1).

4. Discussion

4.1 Controls on evapotranspiration reduction.

The reduction in evapotranspiration following fire was strongly correlated with burn severity and pre-fire vegetation density (Fig. 4). These patterns are consistent with biophysical processes (Bart et al. 2020; Poon and Kinoshita 2018b), though they may also in part reflect correlations between NDVI, evapotranspiration and NBR, as each incorporates Near Infrared reflectance in their calculation. We explored the likelihood of these possible mathematical artifacts by considering both aET and rET , and also by using the five-year-average pre-fire NDVI ($bNDVI$) as a predictor of pre-fire conditions. In principle, rET would be expected to be less mathematically correlated with $bNDVI$ than would aET , and a five-year $bNDVI$ would be expected to be less mathematically correlated with aET than would a one-year $bNDVI$. We observed consistent results across all analyses (Fig. 5, 6), implying that our main findings primarily reflect biophysical processes rather than underlying mathematical dependencies.

Our study corroborates previous watershed-based observations of the ET response to wildfire, and extends these analyses over broader areas, while also relating the results to environmental attributes. Both Roche et al. (2018) and Poon and Kinoshita (2018b) found fire-induced evapotranspiration reduction increased from low to high burn severity. Roche et al. (2018) also reported that the fire-induced evapotranspiration reduction was greatest in denser forests with larger pre-fire basal areas.

The largest absolute ET reductions (aET) occurred in locations where severe wildfires burned in dense forests (Ghazoul et al. 2015; Seidl et al. 2016; Seidl et al. 2017). These regions occur in wetter areas ($P > 1000 \text{ mm yr}^{-1}$; Fig. 5), where sufficient water is available to support high primary productivity (Bales et al. 2018; Goulden and Bales 2014). Non-forested vegetation types, including shrubland and herbaceous communities, had lower aET s and rET s than forests, which is consistent with their less-dense pre-fire canopies and lower rates of pre-fire ET (Fig. S6, Fig. 5). Evergreen forest

(mainly montane mixed-conifer) was the dominant burned vegetation type (57%), which exhibited the largest *aET* (324 mm on average) and *rET* (52% on average) reductions among the five vegetation types considered (Fig. S6). Mixed forest (consisting of hardwoods and conifers) also experienced high *aETs* and *rETs*, but accounted for a small fraction (4%) of the burned area. The *aET* and *rET* in deciduous forest (mainly oak species) was significantly lower than that in other forest types, probably due to lower tree mortality and more rapid recovery (Cocking et al. 2014; Nemens et al. 2018; Varner et al. 2016). Most oak species in California survive wildfire and are able to subsequently resprout; this allows mature plants to maintain deep rooting systems and rapidly regrow dense canopies after fire. Conifers are unable to resprout and must reestablish canopy cover and root systems by regenerating new individual from seed. This is also consistent with the forest type transition after wildfires, in which 66% trees survived in deciduous forests, whereas only 54% remained as evergreen forests (Table. S2). A more-rapid recovery by resprouting species has been reported in other ecosystems, including Eucalyptus forest (Nolan et al. 2015).

The responses of *aET* and *rET* to wildfire were similar across elevation and temperature (Fig. 6), with peaks in the mid-elevation and mid-temperature belt. This zone coincides with the highest rates of primary production and biomass (Goulden and Bales 2019), and also has a comparatively high rate of wildfire (Miller et al. 2012). Higher elevations tend to have reduced primary production and less-severe fire weather, leading to less-frequent wildfire. Warmer conditions occur at lower elevations, which are too dry to support dense canopies (Bales et al. 2011; Bales et al. 2006). Some exceptions exist at higher elevations (>2000 m), where *rET* increased slightly in the severely burned areas (>75% basal area). The increased *rET* (>50%) in those higher-elevation areas reflects forest that is particularly vulnerable to extensive high-severity fire effects (Ghazoul et al. 2015; Seidl et al. 2016; Seidl et al. 2017). The vegetation at higher elevation includes Subalpine Conifer, Lodgepole Pine, Red Fir, and Jeffery Pine, according to the tree type in the Wildlife Habitat Relationships classification system from Calveg dataset <https://www.fs.usda.gov/detail/r5/landmanagement/resourcemanagement/?cid=stelprdb5347192>. These forests have less biomass and leaf area than mid-elevation forests, and are historically

associated with longer fire-return intervals and greater proportions of stand-replacing fire (Fites-Kaufman et al. 2007). These forests also experience a slower recovery from fire (Meng et al. 2015) due to energy limitations, leading to a comparatively greater ET reduction with fire.

Neither slope nor aspect was significantly correlated with ET reduction (Fig. 4 and Fig. S7). This finding diverges from some site-level or basin studies, where aspect and/or slope impacted the ET response through its influence on radiation, moisture, and vegetation growth (Bart et al. 2016; Ebel 2013; Kinoshita and Hogue 2011; Nolan et al. 2015). Regional studies of the impact of large wildfires have shown relatively weak relationships with slope and/or aspect, as high-severity fire often occur across a range of topographic settings; Moreover, the relatively coarse spatial unit in this study (200 m) may also mute the relationships observed in at smaller scale basal-level studies. The impacts of topography at the regional level are often marginal, and mainly associated with initial vegetation density and ET (Hallema et al. 2018b).

4.2 Recent wildfire-driven trends in

evapotranspiration. The total area burned across the Sierra Nevada was 78% higher in 2001-2017 relative to 1985-2000, coincident with warming and drought (Fig. 2). Moreover, the area burned at high severity in 2001-2017 was 2.6 times that in 1985-2000. Similar trends have been reported across the Western United States (Dennison et al. 2014; Miller and Safford 2012; Westerling 2016). These increases have been attributed to overly dense forests with a buildup of surface and ladder fuels (Stephens et al. 2012; Stephens et al. 2009; Stevens et al. 2017; Tubbesing et al. 2019), and a longer fire season with drier and warmer summers and earlier spring snowmelt (Westerling et al. 2006).

The Sierra-wide evapotranspiration reduction from wildfire shows an increasing trend (0.003 bm^3/yr , p value= 0.034, Fig. 2 and Fig. S8a) from 1985 to 2017 reflecting both increasing burned area (Fig. S8b) and more-severe burns (Fig. S8c), with large inter-annual variation. Fire impacts on Sierra Nevada forests and hydrology are projected to increase further with a climate warming (Liang et al. 2017) and further accumulation of fuel (Hurteau et al. 2019; Stephens et al. 2018).

4.3 Sensitivity of evapotranspiration to possible increases in fire occurrence. We used the multi-variable regression analysis to estimate the Sierra Nevada-wide changes in evapotranspiration that would be expected for three possible changes in future fire occurrence. We focused on a 15-year future fire return interval, which approximates the historical fire-return frequency in the mixed-conifer region of our study area, i.e. 12 years reported by Safford and Van de Water (2014); Scholl and Taylor (2010). Our simulation indicates a reintroduction of low-intensity burning or light mechanical thinning (<25% basal area reduction) would have the smallest effect (4.4 ± 0.9 billion $\text{m}^3 \text{yr}^{-1}$ equivalent to 118 ± 24 mm/yr over the restorable areas) on ET (Fig. S5, Table S1) (Bart 2016; Saksa et al. 2017). Comparing to the low-intensity burning, the evapotranspiration reduction would increase by 19% with more-intensive management (25-75% basal area reduction) (Safford and Stevens 2017), and another 23% with a large increase in severe wildfire (>75% basal area reduction).

A large increase in high-severity wildfires would have detrimental impacts on human communities (Stephens et al. 2018), wildlife habitat, and carbon stocks (Spies et al. 2012; Stephens et al. 2018; Stephens et al. 2016). Additionally, increases in high-severity fire effects would likely lead to erosion, reservoir sedimentation, and reduced water quality (Collins et al. 2017b; Ghazoul et al. 2015; Seidl et al. 2017). The result is a tradeoff, with severe fires reducing evapotranspiration and potentially increasing runoff and water yield, along with a suite of potentially deleterious effects. The management challenge is to balance these effects, and to design practices that simultaneously reduced wildfire probability and severity, protect habitat, carbon stocks and water quality and maximize runoff (Liang et al. 2018; North et al. 2015; North et al. 2012). Practically, forest restoration can be limited by cost, accessibility, and ownership, which may limit the area and pace of restoration (Lydersen et al. 2019; North et al. 2015). We found that much of the evapotranspiration reduction (equivalent to $8 \pm 1\%$ of the current annual evapotranspiration) occurs even in low-severity fires, implying that less-severe treatments may provide a meaningful increase in water yields (Saksa et al. 2020; Saksa et al. 2017).

4.4 Limitations and future research needs.

Our analysis could be expanded in three directions. First is consideration of site-based observations or process-based modeling to cross-validate and further explore our results. Second, subsetting the data would allow consideration of the longer-term evapotranspiration recovery and the variation caused by further environmental attributes. Third, our approach provides a foundation for considering changes in additional ecosystem properties and services following disturbance.

We used data-driven ET estimates to evaluate the effects of wildfires. This method has been successfully applied across the Sierra Nevada in previous studies (Goulden et al. 2012; Goulden and Bales 2019; Roche et al. 2018), but limitations nonetheless exist in predicting ET. The RMSE (108 mm/year) of our ET estimation, was not large compared to the errors in model simulated ET reported by Chen et al. (2016) and Blount et al. (2020), which varied from 11 to 27 mm/month depending on vegetation types of flux-tower sites. The variations among vegetation type was consistent with Chen et al. (2016) in that forest sites (175 mm/year) have larger errors than grassland (45mm/year) and shrubland (50 mm/year), as less of the ET calibration data are from dense forest sites (Fig. S1). The mean bias error in our study was -36 mm/year in unburned sites, and 29 mm/year in burned sites, which could underestimate the ET reduction after wildfires by 65mm/year. These magnitude of bias are smaller than modeled results in Blount et al. (2020); Poon and Kinoshita (2018b), which overestimated the ET reduction by approximately 111 mm/year. Quantifying runoff changes associated with reductions in ET is critical for predicting water supply. Using a similar ET estimation model, Roche et al. (2020) projected a 10% increase in runoff after 50% of basal area reduction in two Northern Sierra Nevada basins. These changes in runoff depend on vegetation type, hydrologic condition, and climate, and thus may vary substantially over the Sierra Nevada basins.

Moreover site-level observations (Alfaro-Sánchez et al. 2015; Dore et al. 2012; Nolan et al. 2014a) and process-based hydroecological models (Komatsu and Kume 2020) can better interpret the biophysical mechanisms by partitioning ET, and by analyzing the effects of vegetation loss and recovery (Goeking and Tarboton 2020; Kinoshita and Hogue 2015; Komatsu and Kume 2020). Some previous

studies have concluded that canopy loss has a marginal impact on ET, either due to increased subcanopy radiation and evaporation, and/or rapid post disturbance recovery (Bennett et al. 2018; Biederman et al. 2015; Goeking and Tarboton 2020). Cross-comparing results between data-driven and physically based modeling studies may prove useful for reconciling these results, while bringing deeper insights into how and why ET is affected by wildfire (Bart et al. 2016; Federer and Lash 1978).

We focused on a 15-year post-fire window, whereas a full recovery to pre-fire ET levels may require longer (Fig. 3). This recovery may vary with climate, vegetation type and ecological processes, such as competition or facilitation (Meng et al. 2015; Yang et al. 2017); knowledge of the longer-term effects of fire on vegetation water use is important for planning forest restoration and water management (Tubbesing et al. 2019; van Mantgem et al. 2011; Vernon et al. 2018).

Finally, similar analyses are needed to look at the effects of fire and management on other ecosystem services. Fire effects on forest ecosystems are multifaceted, including reduced carbon stocks (DORE et al. 2008; Murphy et al. 2019), altered wildlife habitat (Stephens et al. 2019) and forest energy balance (Amiro et al. 2006), and degraded water quality (Hallema et al. 2018a). The recovery of some of these properties, such as biomass pools, may be comparatively slow (Amiro et al. 2010). Likewise, analyses of actual management projects are needed. Additional factors may impact the ET after forest treatments, including changes in biomass, density, tree size and species composition can influence the post-treatment transpiration (Bart et al. 2016; Roche et al. 2018;

Saksa et al. 2020; Saksa et al. 2017); treatment methods (mechanical thinning, clear cutting, with/without prescribed fires) and removing versus leaving woody debris on the ground can change evaporation demand by altering the land surface albedo and wetness (Knapp et al. 2017; Stephens and Moghaddas 2005; Walker et al. 2006).

5. Conclusions

Wildfires in California's Sierra Nevada during 1985-2017 reduced vegetation water use by an average of 265 mm yr⁻¹ (36% of pre-fire ET) in the first year following fire, and 169 mm yr⁻¹ (23%) averaged over the first 15 years following fire. The decline in evapotranspiration increased with fire severity and pre-fire vegetation biomass. Dense, mid-elevation, evergreen forests exhibited the largest evapotranspiration decline following wildfire. We used the observed changes in ET following fire to explore the effects of possible widespread forest restoration efforts. This data-driven analysis revealed a 9% ET reduction if 27% of the Sierra Nevada received a treatment equivalent to a moderate severity burn, underscoring the possibility that ecological restoration may simultaneously reduce ET and drought stress and increase water yield, in addition to previously reported reductions in fire severity.

Acknowledgements:

This research was supported by the National Science Foundation through the Southern Sierra Critical Zone Observatory (EAR-0725097, 1239521, and 1331939), California Climate Investments program through the Strategic Growth Council (CCR20021), UC Water Security and Sustainability Research Initiative (grant no. 13941), and the USDA National Institute of Food and Agriculture, McIntire Stennis project 1022944.

Table 1 Data characteristics and sources.

Attribute	Resolution/Unit	Indication/Equation	Data source
NDVI	30m	$NDVI = \frac{NIR - Red}{NIR + Red}$	Landsat 5,7,8 surface reflectance, GEE, USGS
Vegetation type	30m	NA	NLCD
Elevation	30m	NA	SRTM
Northness	30m	$Northness = \sin(Slope) \times \cos(Aspect)$	SRTM based Slope and Aspect
Precipitation	800m	annual total precipitation	PRISM
Temperature	800m	annual mean temperature	PRISM
Fire severity	30m	7 fire severity classes	Vegetation burn severity, USFS
Fire size	km ²	area of each fire	Perimeters of fires, USFS
dNBR	30m	$NBR = \frac{NIR - SWIR2}{NIR + SWIR2};$ $dNBR = NBR_{prefire} - NBR_{postfire}$	MTBS
RdNBR	30m	$RdNBR = \frac{dNBR}{\sqrt{ NBR_{prefire}/1000 }}$	MTBS

dNBR (Delta Normalized Burn Ratio) and RdNBR (Relative differenced Normalized Burn Ratio) are burn severity indices calculated from Landsat imagery. NIR (near infrared), Red, and SWIR2 (shortwave infrared band2) are surface reflectance bands for NDVI, dNBR, RdNBR calculation. GEE (Google Earth Engine) and USGS (US Geological Survey), NLCD (National Land Cover Database), SRTM (Shuttle Radar Topography Mission), PRISM (Parameter-elevation Regressions on Independent Slopes Model), USFS (US forest service), and MTBS (Monitoring Trends in Burn Severity) are data sources.

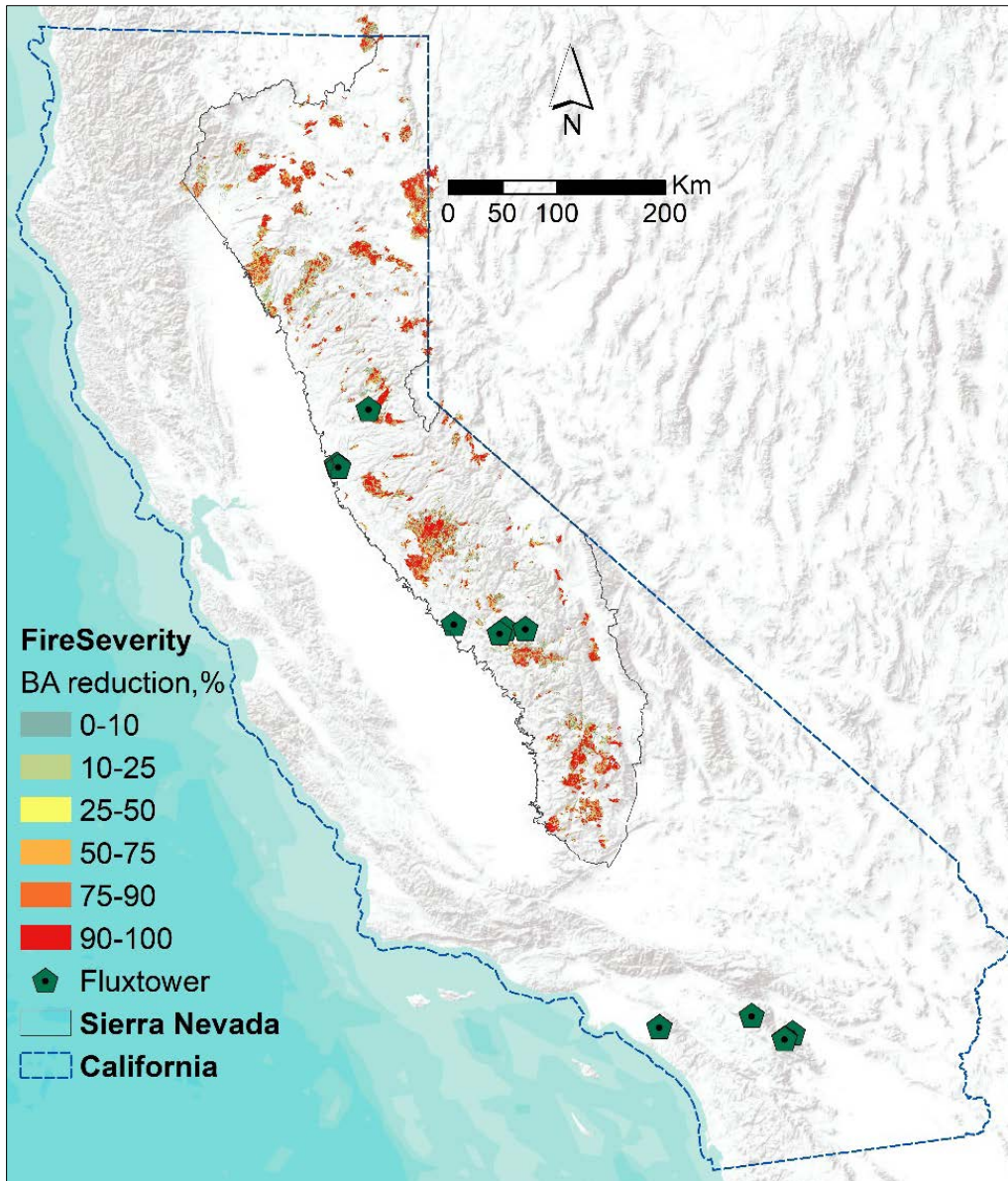


Fig. 1 Distribution of fire perimeters and severities (defined as percentage of basal area, BA, reduction) in the study area. The fire burn severity data are provided by USDA Forest Service fire and fuels monitoring project, collected from 1985 to 2017. The flux tower includes 12 sites all over the California, which were used to simulate the annual ET in the Sierra Nevada study area with Landsat imagery and precipitation data.

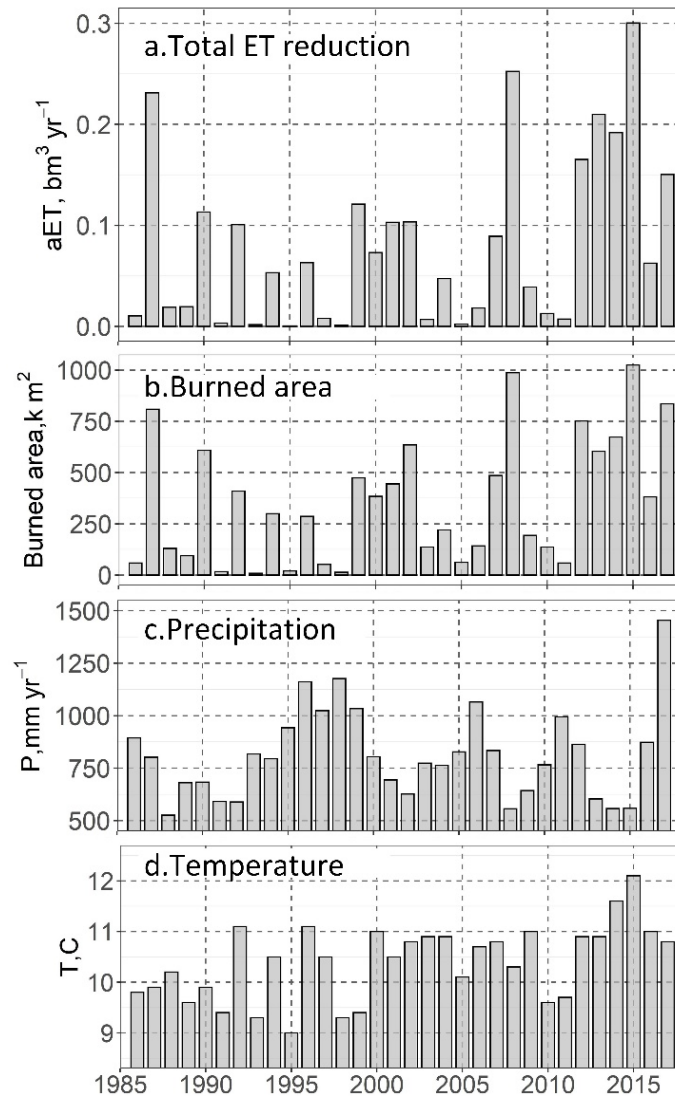


Fig. 2 The Sierra Nevada wide annual a) ET reduction, b) fire-impacted area, c) water-year precipitation and d) water-year mean temperature. The total ET reduction (aET) is calculated as the ET reduction in the first year post-fire using Equation 1, over all the areas burned in each year from 1986 to 2017. The water-year is calculated from October 1 to September 30.

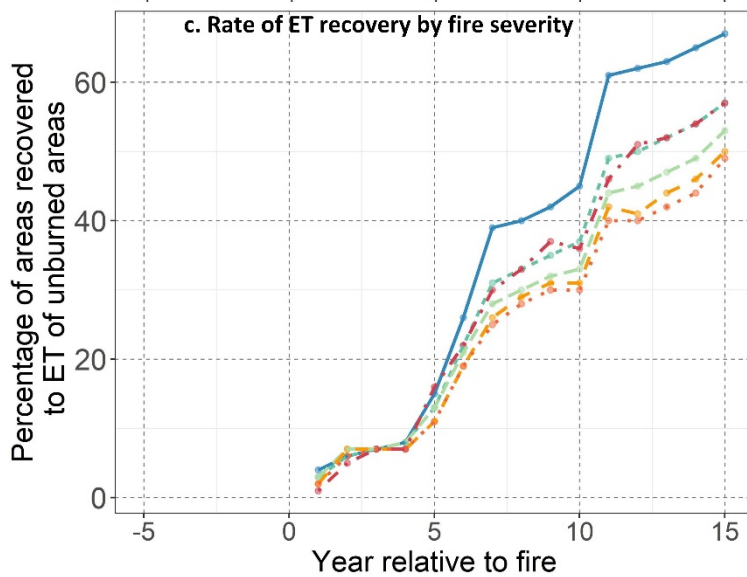
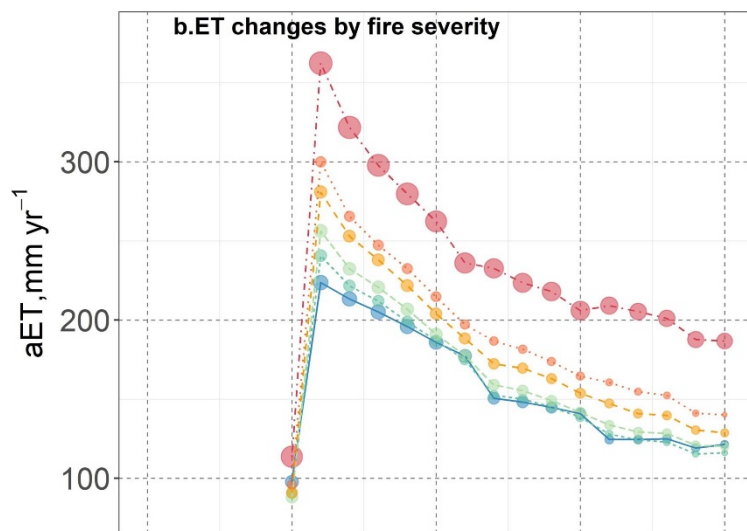
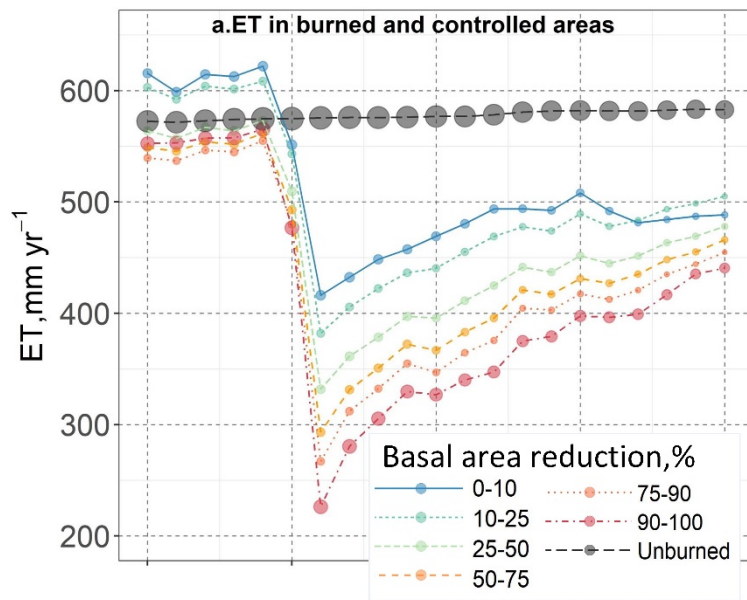


Fig. 3 a) Evapotranspiration (ET) averaged over all fires across the Sierra Nevada at burned and corresponding unburned areas from 5 years before to 15 years after fire. b) Absolute evapotranspiration reduction (aET) averaged over all fires for 15 years after fire. c) Percent of areas with ET recovery to levels of unburned control areas for 15 years after fire. Values are grouped by fire severity across all 635 fires that occurred during 1986-2017. Dot size is proportional to the area in each statistic.

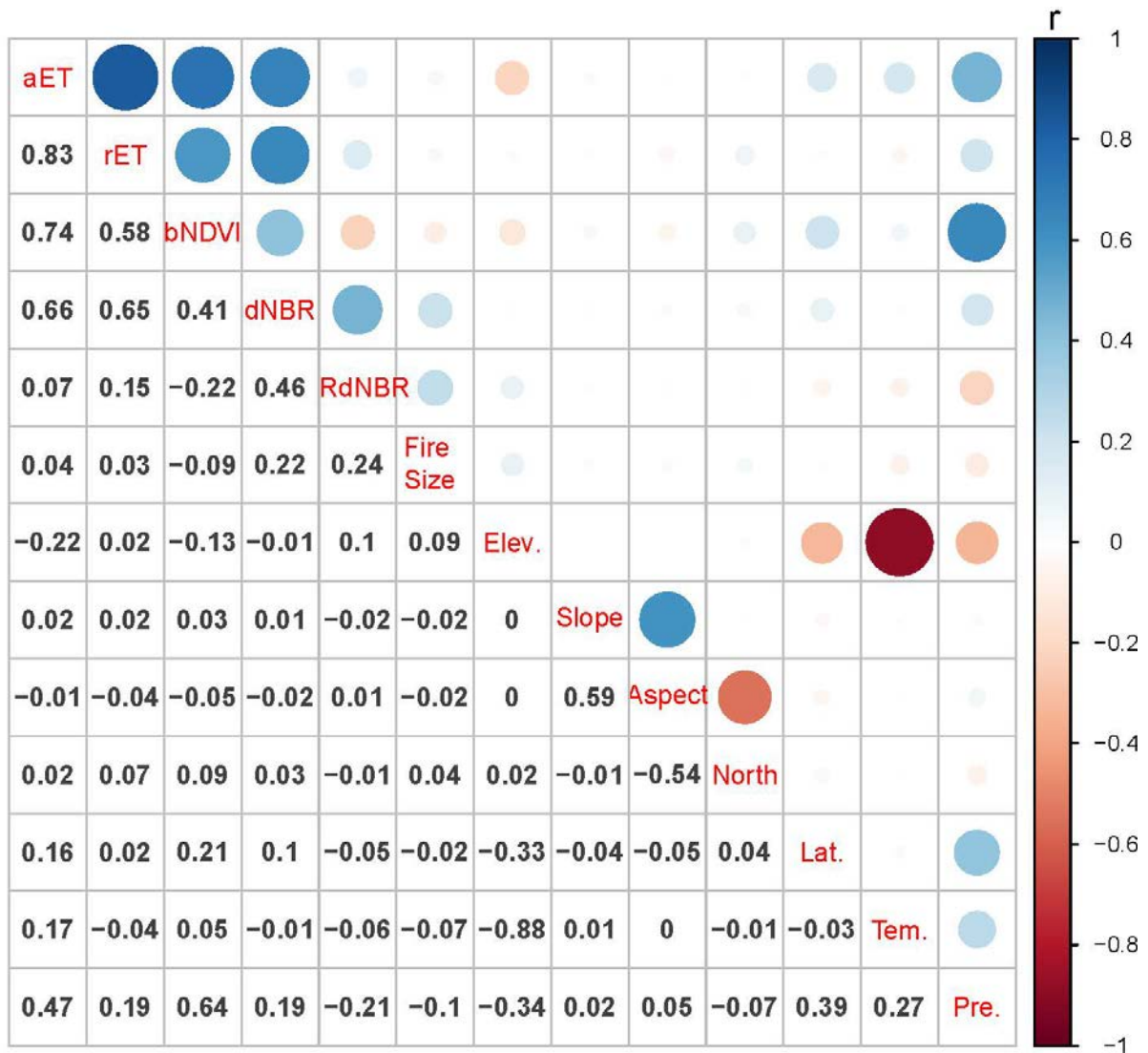


Fig. 4 The matrix of correlations between evapotranspiration reduction in absolute (aET) and relative (rET) values and eleven environmental attributes, plus the correlations among them. bNDVI is the five-year-average pre-fire NDVI. RdNBR and dNBR are fire indices standing for Relative differenced Normalized Burn Ratio and delta Normalized Burn Ratio, respectively. North is the Northness. Lat. is the latitude. Tem. and Pre. are the normal-year mean temperature and total precipitation from Parameter-elevation Regressions on Independent Slopes Model 800 m dataset, respectively.

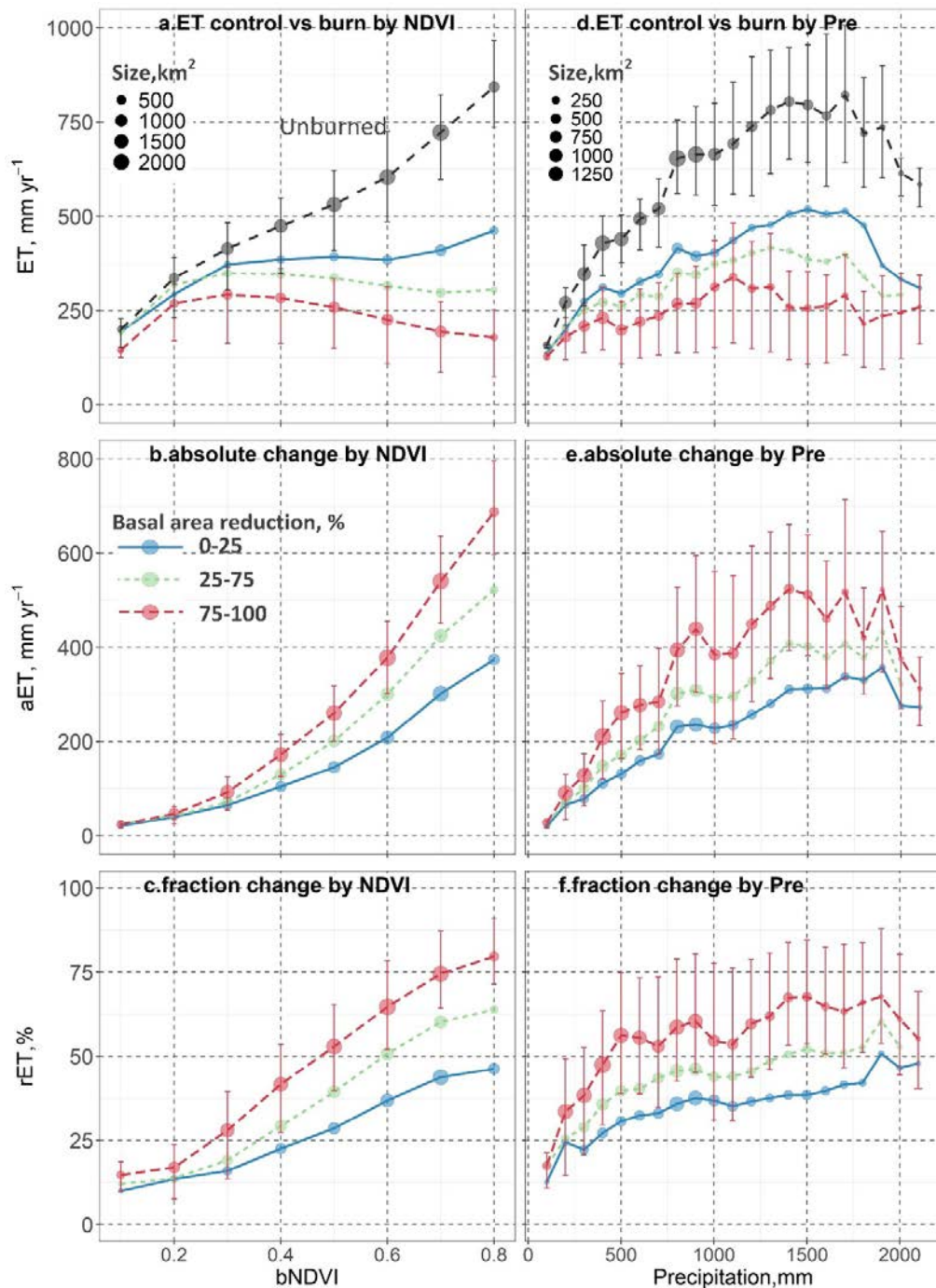


Fig. 5 Evapotranspiration (ET) response to fires of three burn severities by pre-fire NDVI and precipitation: (a,d) ET in unburned control and burned areas in the first year after the fire, (b,e) absolute evapotranspiration reduction (aET) in the first-year post-fire, and (c,f) fraction of ET reduction relative to pre-fire (rET). The values presented are means of burned area at three aggregated fire-severity classes (low: 0-25%, moderate: 25-75%, high: 75-100% basal area reduction) over 1986-2017, in 100-mm normal annual precipitation bins and 0.1 unit of NDVI bins. Dot size is proportional to the fire-impacted area and corresponding unburned area. The error bars represent the 25%-75% value range of areas burned with 75-100% basal area reduction (the fire-severity class with largest burned area) and controlled areas.

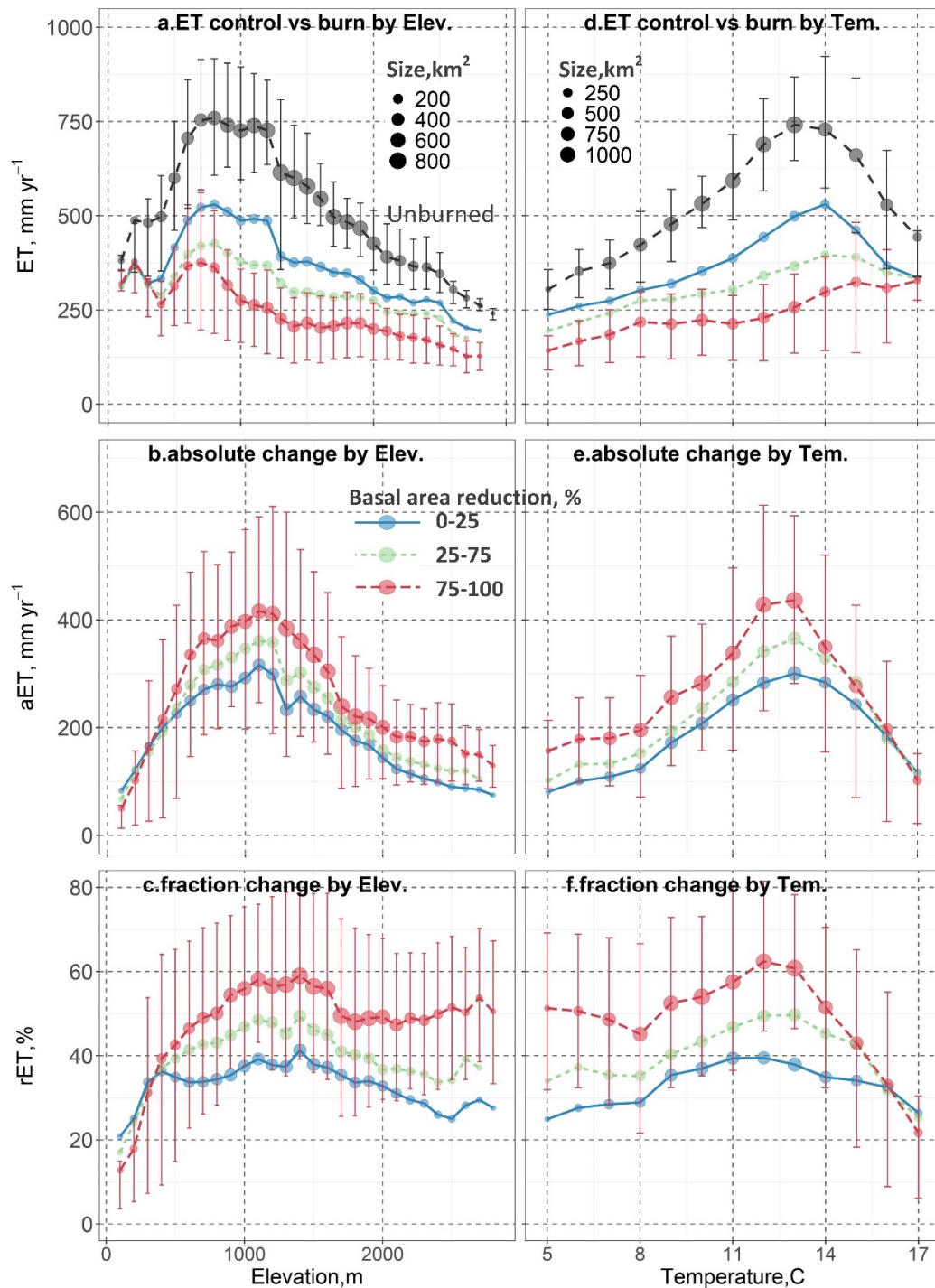


Fig. 6 Evapotranspiration (ET) response to fires of three burn severities by Elevation (DEM) and Temperature (T): (a,d) ET in unburned control and burned areas in the first year after the fire, (b,e) absolute evapotranspiration reduction (aET) in the first-year post-fire, and (c,f) fraction of ET reduction relative to pre-fire (rET). The values presented are means of burned area at three aggregated fire-severity classes (low: 0-25%, moderate: 25-75%, high:75-100% basal area reduction) over 1986-2017, in 100-m elevation bins and 1 °C temperature bins. Dot size is proportional to the fire-impacted area and corresponding unburned area. The error bars represent the 25%-75% value range of areas burned with 75-100% basal area reduction (the fire-severity class with largest burned area) and controlled areas.

References

- Alfaro-Sánchez, R., R. Sánchez-Salguero, J. De las Heras, E. Hernández-Tecles, D. Moya & F. R. López-Serrano, 2015. Vegetation dynamics of managed Mediterranean forests 16 yr after large fires in southeastern Spain. *Applied Vegetation Science* 18(2):272-282 doi:10.1111/avsc.12137.
- Amiro, B. D., A. G. Barr, J. G. Barr, T. A. Black, R. Bracho, M. Brown, J. Chen, K. L. Clark, K. J. Davis, A. R. Desai, S. Dore, V. Engel, J. D. Fuentes, A. H. Goldstein, M. L. Goulden, T. E. Kolb, M. B. Lavigne, B. E. Law, H. A. Margolis, T. Martin, J. H. McCaughey, L. Misson, M. Montes-Helu, A. Noormets, J. T. Randerson, G. Starr & J. Xiao, 2010. Ecosystem carbon dioxide fluxes after disturbance in forests of North America. *Journal of Geophysical Research: Biogeosciences* 115(G4) doi:10.1029/2010jg001390.
- Amiro, B. D., A. L. Orchansky, A. G. Barr, T. A. Black, S. D. Chambers, F. S. Chapin III, M. L. Goulden, M. Litvak, H. P. Liu, J. H. McCaughey, A. McMillan & J. T. Randerson, 2006. The effect of post-fire stand age on the boreal forest energy balance. *Agricultural and Forest Meteorology* 140(1):41-50 doi:<https://doi.org/10.1016/j.agrformet.2006.02.014>.
- Andréassian, V., 2004. Waters and forests: from historical controversy to scientific debate. *Journal of hydrology* 291(1-2):1-27 doi:10.1016/j.jhydrol.2003.12.015.
- Bales, R. C., J. J. Battles, Y. Chen, M. H. Conklin, E. Holst, K. L. O'Hara, P. Saksa & W. Stewart, 2011. Forests and water in the Sierra Nevada: Sierra Nevada watershed ecosystem enhancement project. Sierra Nevada Research Institute report(11.1).
- Bales, R. C., M. L. Goulden, C. T. Hunsaker, M. H. Conklin, P. C. Hartsough, A. T. O'Geen, J. W. Hopmans & M. Safeeq, 2018. Mechanisms controlling the impact of multi-year drought on mountain hydrology. *Scientific Reports* 8(1):690 doi:10.1038/s41598-017-19007-0.
- Bales, R. C., N. P. Molotch, T. H. Painter, M. D. Dettinger, R. Rice & J. Dozier, 2006. Mountain hydrology of the western United States. *Water Resources Research* 42(8) doi:10.1029/2005WR004387.
- Bart, R. R., 2016. A regional estimate of postfire streamflow change in California. *Water Resources Research* 52(2):1465-1478 doi:10.1002/2014WR016553.
- Bart, R. R., M. C. Kennedy, C. L. Tague & D. McKenzie, 2020. Integrating fire effects on vegetation carbon cycling within an ecohydrologic model. *Ecol Model* 416:108880 doi:<https://doi.org/10.1016/j.ecolmodel.2019.108880>.
- Bart, R. R., C. L. Tague & M. A. Moritz, 2016. Effect of Tree-to-Shrub Type Conversion in Lower Montane Forests of the Sierra Nevada (USA) on Streamflow. *PloS one* 11(8):e0161805-e0161805 doi:10.1371/journal.pone.0161805.
- Battles, J. J., D. M. Bell, R. E. Kennedy, D. S. Saah, B. M. Collins, R. A. York, J. E. Sanders & F. Lopez-Ornelas, 2018. Innovations in measuring and managing forest carbon stocks in California. California's Fourth Climate Change Assessment, California Natural Resources Agency. Publication number: CNRACCC4A-2018-XXX, Sacramento, CA.
- Bennett, K. E., T. J. Bohn, K. Solander, N. G. McDowell, C. Xu, E. Vivoni & R. S. Middleton, 2018. Climate-driven disturbances in the San Juan River sub-basin of the Colorado River. *Hydrology and Earth System Sciences (Online)* 22(PNNL-SA-129830; LA-UR-17-27609) doi:<https://doi.org/10.5194/hess-22-709-2018>.
- Biederman, J. A., A. J. Somor, A. A. Harpole, E. D. Gutmann, D. D. Breshears, P. A. Troch, D. J. Gochis, R. L. Scott, A. J. Meddens & P. D. Brooks, 2015. Recent tree die-off has little effect on streamflow in contrast to expected increases from historical studies. *Water Resources Research* 51(12):9775-9789 doi:10.1002/2015WR017401.
- Blount, K., C. J. Ruybal, K. J. Franz & T. S. Hogue, 2020. Increased water yield and altered water partitioning follow wildfire in a forested catchment in the western United States. *Ecohydrology* 13(1):e2170 doi:10.1002/eco.2170.
- Boisramé, G., S. Thompson, B. Collins & S. Stephens, 2017. Managed wildfire effects on forest resilience and water in the Sierra Nevada. *Ecosystems* 20(4):717-732 doi:<https://doi.org/10.1007/s10021-016-0048-1>.
- Boisramé, G., S. Thompson & S. Stephens, 2018. Hydrologic responses to restored wildfire regimes revealed by soil moisture-vegetation relationships. *Advances in Water Resources* 112:124-146 doi:<https://doi.org/10.1016/j.advwatres.2017.12.009>.
- Boisramé, G. F. S., S. E. Thompson, C. Tague & S. L. Stephens, 2019. Restoring a Natural Fire Regime Alters the Water Balance of a Sierra Nevada Catchment. *Water Resources Research* 0(ja) doi:10.1029/2018wr024098.
- Breiman, L., 2001. Random forests. *Mach Learn* 45 doi:10.1023/a:1010933404324.
- Chen, M., G. B. Senay, R. K. Singh & J. P. Verdin, 2016. Uncertainty analysis of the Operational Simplified Surface Energy Balance (SSEBop) model at multiple flux tower sites. *Journal of Hydrology* 536:384-399 doi:<https://doi.org/10.1016/j.jhydrol.2016.02.026>.
- Cocking, M. I., J. M. Varner & E. E. Knapp, 2014. Long-term effects of fire severity on oak-conifer dynamics in the southern Cascades. *Ecol Appl* 24(1):94-107 doi:10.1890/13-0473.1.
- Collins, B. M., R. G. Everett & S. L. Stephens, 2011. Impacts of fire exclusion and recent managed fire on forest structure in old growth Sierra Nevada mixed-conifer forests. *Ecosphere* 2(4):1-14 doi:10.1890/ES11-00026.1.
- Collins, B. M., D. L. Fry, J. M. Lydersen, R. Everett & S. L. Stephens, 2017a. Impacts of different land management histories on forest change. *Ecol Appl* 27(8):2475-2486 doi:<https://doi.org/10.1002/eap.1622>.
- Collins, B. M., J. M. Lydersen, R. G. Everett & S. L. Stephens, 2018. How does forest recovery following moderate-severity fire influence effects of subsequent wildfire in mixed-conifer forests? *Fire Ecology* 14(2):3 doi:10.1186/s42408-018-0004-x.
- Collins, B. M., J. T. Stevens, J. D. Miller, S. L. Stephens, P. M. Brown & M. P. North, 2017b. Alternative characterization of forest fire regimes: incorporating spatial patterns. *Landscape Ecol* 32(8):1543-1552 doi:10.1007/s10980-017-0528-5.
- Dennison, P. E., S. C. Brewer, J. D. Arnold & M. A. Moritz, 2014. Large wildfire trends in the western United States, 1984-2011. *Geophys Res Lett* 41(8):2928-2933 doi:10.1002/2014GL059576.
- DORE, S., T. E. KOLB, M. MONTES-HELU, B. W. SULLIVAN, W. D. WINSLOW, S. C. HART, J. P. KAYE, G. W. KOCH & B. A. HUNGATE, 2008. Long-term impact of a stand-replacing fire on ecosystem CO₂ exchange of a ponderosa pine forest. *Global Change Biol* 14(8):1801-1820 doi:10.1111/j.1365-2486.2008.01613.x.
- Dore, S., M. Montes-Helu, S. C. Hart, B. A. Hungate, G. W. Koch, J. B. Moon, A. J. Finkral & T. E. Kolb, 2012. Recovery of ponderosa pine ecosystem carbon and water fluxes from thinning and stand-replacing fire. *Global Change Biol* 18(10):3171-3185 doi:10.1111/j.1365-

- 2486.2012.02775.x.
- Ebel, B. A., 2013. Simulated unsaturated flow processes after wildfire and interactions with slope aspect. *Water Resources Research* 49(12):8090-8107 doi:10.1002/2013wr014129.
- Federer, C. A. & D. Lash, 1978. Simulated streamflow response to possible differences in transpiration among species of hardwood trees. *Water Resources Research* 14(6):1089-1097 doi:10.1029/WR014i006p01089.
- Fites-Kaufman, J. A., P. Rundel, N. Stephenson & D. A. Weixelman, 2007. Montane and Subalpine Vegetation of the Sierra Nevada and Cascade Ranges. In Barbour, M. G., T. Keeler-Wolf & A. A. Schoenherr (eds) *Terrestrial Vegetation of California*, 3rd Edition. 1 edn. University of California Press, 456-501.
- Ghazoul, J., Z. Burivalova, J. Garcia-Ulloa & L. A. King, 2015. Conceptualizing Forest Degradation. *Trends Ecol Evol* 30(10):622-632 doi:<https://doi.org/10.1016/j.tree.2015.08.001>.
- Goeking, S. A. & D. G. Tarboton, 2020. Forests and Water Yield: A Synthesis of Disturbance Effects on Streamflow and Snowpack in Western Coniferous Forests. *J For* 118(2):172-192 doi:10.1093/jofore/fvz069.
- Goulden, M. L., R. G. Anderson, R. C. Bales, A. E. Kelly, M. Meadows & G. C. Winston, 2012. Evapotranspiration along an elevation gradient in California's Sierra Nevada.
- Goulden, M. L. & R. C. Bales, 2014. Mountain runoff vulnerability to increased evapotranspiration with vegetation expansion. *Proceedings of the National Academy of Sciences* 111(39):14071-14075 doi:10.1073/pnas.1319316111.
- Goulden, M. L. & R. C. Bales, 2019. California forest die-off linked to multi-year deep soil drying in 2012–2015 drought. *Nature Geoscience* doi:10.1038/s41561-019-0388-5.
- Hallema, D. W., F.-N. Robinne & K. D. Bladon, 2018a. Reframing the Challenge of Global Wildfire Threats to Water Supplies. *Earth's Future* 6(6):772-776 doi:10.1029/2018EF000867.
- Hallema, D. W., G. Sun, P. V. Caldwell, S. P. Norman, E. C. Cohen, Y. Liu, K. D. Bladon & S. G. McNulty, 2018b. Burned forests impact water supplies. *Nature Communications* 9(1):1307 doi:10.1038/s41467-018-03735-6.
- Hallema, D. W., G. Sun, P. V. Caldwell, S. P. Norman, E. C. Cohen, Y. Liu, E. J. Ward & S. G. McNulty, 2017. Assessment of wildland fire impacts on watershed annual water yield: Analytical framework and case studies in the United States. *Ecohydrology* 10(2):e1794 doi:<https://doi.org/10.1002/eco.1794>.
- Hessburg, P. F., J. K. Agee & J. F. Franklin, 2005. Dry forests and wildland fires of the inland Northwest USA: contrasting the landscape ecology of the pre-settlement and modern eras. *For Ecol Manage* 211(1-2):117-139 doi:10.1016/j.foreco.2005.02.016.
- Hibbert, A. R., 1965. Forest treatment effects on water yield. *Citeseer*.
- Hurteau, M. D., S. Liang, A. L. Westerling & C. Wiedinmyer, 2019. Vegetation-fire feedback reduces projected area burned under climate change. *Scientific Reports* 9(1):2838 doi:10.1038/s41598-019-39284-1.
- Jin, S., Y. Su, S. Gao, T. Hu, J. Liu & Q. Guo, 2018. The Transferability of Random Forest in Canopy Height Estimation from Multi-Source Remote Sensing Data. *Remote Sensing* 10(8):1183.
- Jin, Y., J. T. Randerson & M. L. Goulden, 2011. Continental-scale net radiation and evapotranspiration estimated using MODIS satellite observations. *Remote Sens Environ* 115(9):2302-2319 doi:10.1016/j.rse.2011.04.031.
- Kinoshita, A. M. & T. S. Hogue, 2011. Spatial and temporal controls on post-fire hydrologic recovery in Southern California watersheds. *CATENA* 87(2):240-252 doi:<https://doi.org/10.1016/j.catena.2011.06.005>.
- Kinoshita, A. M. & T. S. Hogue, 2015. Increased dry season water yield in burned watersheds in Southern California. *Environmental Research Letters* 10(1):014003 doi:10.1088/1748-9326/10/1/014003.
- Knapp, E. E., J. M. Lydersen, M. P. North & B. M. Collins, 2017. Efficacy of variable density thinning and prescribed fire for restoring forest heterogeneity to mixed-conifer forest in the central Sierra Nevada, CA. *For Ecol Manage* 406:228-241 doi:<https://doi.org/10.1016/j.foreco.2017.08.028>.
- Knapp, E. E., C. N. Skinner, M. P. North & B. L. Estes, 2013. Long-term overstory and understory change following logging and fire exclusion in a Sierra Nevada mixed-conifer forest. *For Ecol Manage* 310:903-914 doi:<http://dx.doi.org/10.1016/j.foreco.2013.09.041>.
- Komatsu, H. & T. Kume, 2020. Modeling of evapotranspiration changes with forest management practices: a genealogical review. *Journal of Hydrology*:124835 doi:<https://doi.org/10.1016/j.jhydrol.2020.124835>.
- Li, X., Y. He, Z. Zeng, X. Lian, X. Wang, M. Du, G. Jia, Y. Li, Y. Ma, Y. Tang, W. Wang, Z. Wu, J. Yan, Y. Yao, P. Ciais, X. Zhang, Y. Zhang, Y. Zhang, G. Zhou & S. Piao, 2018. Spatiotemporal pattern of terrestrial evapotranspiration in China during the past thirty years. *Agricultural and Forest Meteorology* 259:131-140 doi:<https://doi.org/10.1016/j.agrformet.2018.04.020>.
- Liang, S., M. D. Hurteau & A. L. Westerling, 2017. Potential decline in carbon carrying capacity under projected climate-wildfire interactions in the Sierra Nevada. *Scientific Reports* 7(1):2420 doi:10.1038/s41598-017-02686-0.
- Liang, S., M. D. Hurteau & A. L. Westerling, 2018. Large-scale restoration increases carbon stability under projected climate and wildfire regimes. *Front Ecol Environ* 16(4):207-212 doi:10.1002/fee.1791.
- Liu, Y., M. Kumar, G. G. Katul & A. Porporato, 2019. Reduced resilience as an early warning signal of forest mortality. *Nature Climate Change*:1-6 doi:<https://doi.org/10.1038/s41558-019-0583-9>.
- Lydersen, J. M., B. M. Collins & C. T. Hunsaker, 2019. Implementation constraints limit benefits of restoration treatments in mixed-conifer forests. *Int J Wildland Fire*: doi:<https://doi.org/10.1071/WF18141>.
- Ma, Q., Y. Su, S. Tao & Q. Guo, 2017. Quantifying individual tree growth and tree competition using bi-temporal airborne laser scanning data: a case study in the Sierra Nevada Mountains, California. *International Journal of Digital Earth*:1-19 doi:<http://dx.doi.org/10.1080/17538947.2017.1336578>.
- Meng, R., P. E. Dennison, C. Huang, M. A. Moritz & C. D'Antonio, 2015. Effects of fire severity and post-fire climate on short-term vegetation recovery of mixed-conifer and red fir forests in the Sierra Nevada Mountains of California. *Remote Sens Environ* 171:311-325 doi:<http://dx.doi.org/10.1016/j.rse.2015.10.024>.
- Miller, J. D., B. M. Collins, J. A. Lutz, S. L. Stephens, J. W. van Wagtenonk & D. A. Yasuda, 2012. Differences in wildfires among ecoregions and land management agencies in the Sierra Nevada region, California, USA. *Ecosphere* 3(9):1-20 doi:DOI: 10.1890/ES12-00158.1.

- Miller, J. D., E. E. Knapp, C. H. Key, C. N. Skinner, C. J. Isbell, R. M. Creasy & J. W. Sherlock, 2009. Calibration and validation of the relative differenced Normalized Burn Ratio (RdNBR) to three measures of fire severity in the Sierra Nevada and Klamath Mountains, California, USA. *Remote Sens Environ* 113(3):645-656 doi:10.1016/j.rse.2008.11.009.
- Miller, J. D. & B. Quayle, 2015. Calibration and validation of immediate post-fire satellite-derived data to three severity metrics. *Fire Ecology* 11(2) doi:10.4996/fireecology.1102012.
- Miller, J. D. & H. Safford, 2012. Trends in wildfire severity: 1984 to 2010 in the Sierra Nevada, Modoc Plateau, and southern Cascades, California, USA. *Fire Ecology* 8(3):41-57 doi:10.4996/fireecology.0803041.
- Miller, J. D. & A. E. Thode, 2007. Quantifying burn severity in a heterogeneous landscape with a relative version of the delta Normalized Burn Ratio (dNBR). *Remote Sens Environ* 109(1):66-80 doi:<https://doi.org/10.1016/j.rse.2006.12.006>.
- Murphy, B. P., L. D. Prior, M. A. Cochrane, G. J. Williamson & D. M. J. S. Bowman, 2019. Biomass consumption by surface fires across Earth's most fire-prone continent. *Global Change Biol* 0(ja) doi:10.1111/gcb.14460.
- Nemens, D. G., J. M. Varner, K. R. Kidd & B. Wing, 2018. Do repeated wildfires promote restoration of oak woodlands in mixed-conifer landscapes? *For Ecol Manage* 427:143-151 doi:<https://doi.org/10.1016/j.foreco.2018.05.023>.
- Nolan, R. H., P. N. J. Lane, R. G. Benyon, R. A. Bradstock & P. J. Mitchell, 2014a. Changes in evapotranspiration following wildfire in resprouting eucalypt forests. *Ecohydrology* 7(5):1363-1377 doi:10.1002/eco.1463.
- Nolan, R. H., P. N. J. Lane, R. G. Benyon, R. A. Bradstock & P. J. Mitchell, 2015. Trends in evapotranspiration and streamflow following wildfire in resprouting eucalypt forests. *Journal of Hydrology* 524:614-624 doi:<https://doi.org/10.1016/j.jhydrol.2015.02.045>.
- Nolan, R. H., P. J. Mitchell, R. A. Bradstock & P. N. J. Lane, 2014b. Structural adjustments in resprouting trees drive differences in post-fire transpiration. *Tree Physiology* 34(2):123-136 doi:10.1093/treephys/tpt125.
- North, M., 2012. Managing Sierra Nevada forests. Gen Tech Rep PSW-GTR-237 Albany, CA: US Department of Agriculture, Forest Service, Pacific Southwest Research Station 184 p 237.
- North, M., A. Brough, J. Long, B. Collins, P. Bowden, D. Yasuda, J. Miller & N. Sugihara, 2015. Constraints on mechanized treatment significantly limit mechanical fuels reduction extent in the Sierra Nevada. *J For* 113(1):40-48 doi:<http://dx.doi.org/10.5849/jof.14-058>.
- North, M., B. M. Collins & S. Stephens, 2012. Using fire to increase the scale, benefits, and future maintenance of fuels treatments. *J For* 110(7):392-401 doi:<http://dx.doi.org/10.5849/jof.12-021>.
- Poon, P. K. & A. M. Kinoshita, 2018a. Estimating Evapotranspiration in a Post-Fire Environment Using Remote Sensing and Machine Learning. *Remote Sensing* 10(11):1728 doi:10.3390/rs10111728.
- Poon, P. K. & A. M. Kinoshita, 2018b. Spatial and temporal evapotranspiration trends after wildfire in semi-arid landscapes. *Journal of Hydrology* 559:71-83 doi:<https://doi.org/10.1016/j.jhydrol.2018.02.023>.
- Roche, J. W., M. L. Goulden & R. C. Bales, 2018. Estimating evapotranspiration change due to forest treatment and fire at the basin scale in the Sierra Nevada, California. *Ecohydrology*:e1978 doi:<https://doi.org/10.1002/eco.1978>.
- Roche, J. W., Q. Ma, J. Rungee & R. C. Bales, 2020. Evapotranspiration Mapping for Forest Management in California's Sierra Nevada. *Frontiers in Forests and Global Change* 3(69) doi:10.3389/ffgc.2020.00069.
- Ryu, Y., D. D. Baldocchi, H. Kobayashi, C. Ingen, J. Li, T. A. Black, J. Beringer, E. Gorsel, A. Knohl & B. E. Law, 2011. Integration of MODIS land and atmosphere products with a coupled-process model to estimate gross primary productivity and evapotranspiration from 1 km to global scales. *Global Biogeochemical Cycles* 25(4) doi:10.1029/2011GB004053.
- Safford, H. D. & J. T. Stevens, 2017. Natural range of variation for yellow pine and mixed-conifer forests in the Sierra Nevada, southern Cascades, and Modoc and Inyo National Forests, California, USA. Gen Tech Rep PSW-GTR-256 Albany, CA: US Department of Agriculture, Forest Service, Pacific Southwest Research Station 229 p 256.
- Safford, H. D. & K. M. Van de Water, 2014. Using fire return interval departure (FRID) analysis to map spatial and temporal changes in fire frequency on national forest lands in California. Res Pap PSW-RP-266 Albany, CA: US Department of Agriculture, Forest Service, Pacific Southwest Research Station 59 p 266.
- Saksa, P. C., R. C. Bales, C. L. Tague, J. J. Battles, B. W. Tobin & M. H. Conklin, 2020. Fuels treatment and wildfire effects on runoff from Sierra Nevada mixed-conifer forests. *Ecohydrology* 0(ja):e2151 doi:10.1002/eco.2151.
- Saksa, P. C., M. H. Conklin, J. J. Battles, C. L. Tague & R. C. Bales, 2017. Forest thinning impacts on the water balance of Sierra Nevada mixed-conifer headwater basins. *Water Resources Research* 53(7):5364-5381 doi:10.1002/2016WR019240.
- Scholl, A. E. & A. H. Taylor, 2010. Fire regimes, forest change, and self-organization in an old-growth mixed-conifer forest, Yosemite National Park, USA. *Ecol Appl* 20(2):362-380 doi:10.1890/08-2324.1.
- Seidl, R., T. A. Spies, D. L. Peterson, S. L. Stephens & J. A. Hicke, 2016. REVIEW: Searching for resilience: addressing the impacts of changing disturbance regimes on forest ecosystem services. *J Appl Ecol* 53(1):120-129 doi:10.1111/1365-2664.12511.
- Seidl, R., D. Thom, M. Kautz, D. Martin-Benito, M. Peltoniemi, G. Vacchiano, J. Wild, D. Ascoli, M. Petr, J. Honkaniemi, M. J. Lexer, V. Trotsiuk, P. Mairota, M. Svoboda, M. Fabrika, T. A. Nagel & C. P. O. Reyer, 2017. Forest disturbances under climate change. *Nature Climate Change* 7:395 doi:10.1038/nclimate3303 <https://www.nature.com/articles/nclimate3303#supplementary-information>.
- Spies, T. A., D. B. Lindenmayer, A. M. Gill, S. L. Stephens & J. K. Agee, 2012. Challenges and a checklist for biodiversity conservation in fire-prone forests: Perspectives from the Pacific Northwest of USA and Southeastern Australia. *Biol Conserv* 145(1):5-14 doi:<http://dx.doi.org/10.1016/j.biocon.2011.09.008>.
- Stephens, S. L., B. M. Collins, C. J. Fettig, M. A. Finney, C. M. Hoffman, E. E. Knapp, M. P. North, H. Safford & R. B. Wayman, 2018. Drought, Tree Mortality, and Wildfire in Forests Adapted to Frequent Fire. *Bioscience* doi:10.1093/biosci/bix146.
- Stephens, S. L., L. N. Kobziar, B. M. Collins, R. Davis, P. Z. Fulé, W. Gaines, J. Ganey, J. M. Guldin, P. F. Hessburg, K. Hiers, S. Hoagland, J. J. Keane, R. E. Masters, A. E. McKellar, W. Montague, M. North & T. A. Spies, 2019. Is fire "for the birds"? How two rare species influence fire management across the US. *Front Ecol Environ* 0(0) doi:10.1002/fee.2076.

- Stephens, S. L., J. D. McIver, R. E. J. Boerner, C. J. Fettig, J. B. Fontaine, B. R. Hartsough, P. L. Kennedy & D. W. Schwilk, 2012. The Effects of Forest Fuel-Reduction Treatments in the United States. *Bioscience* 62(6):549-560 doi:[10.1525/bio.2012.62.6.6](https://doi.org/10.1525/bio.2012.62.6.6).
- Stephens, S. L., J. D. Miller, B. M. Collins, M. P. North, J. J. Keane & S. L. Roberts, 2016. Wildfire impacts on California spotted owl nesting habitat in the Sierra Nevada. *Ecosphere* 7(11) doi:[10.1002/ecs2.1478](https://doi.org/10.1002/ecs2.1478).
- Stephens, S. L. & J. J. Moghaddas, 2005. Experimental fuel treatment impacts on forest structure, potential fire behavior, and predicted tree mortality in a California mixed conifer forest. *For Ecol Manage* 215(1):21-36 doi:<https://doi.org/10.1016/j.foreco.2005.03.070>.
- Stephens, S. L., J. J. Moghaddas, C. Edminster, C. E. Fiedler, S. Haase, M. Harrington, J. E. Keeley, E. E. Knapp, J. D. McIver & K. Metlen, 2009. Fire treatment effects on vegetation structure, fuels, and potential fire severity in western US forests. *Ecol Appl* 19(2):305-320 doi:<https://doi.org/10.1890/07-1755.1>.
- Stevens, J. T., B. M. Collins, J. D. Miller, M. P. North & S. L. Stephens, 2017. Changing spatial patterns of stand-replacing fire in California conifer forests. *For Ecol Manage* 406(Supplement C):28-36 doi:<https://doi.org/10.1016/j.foreco.2017.08.051>.
- Su, Y., R. C. Bales, Q. Ma, K. Nydick, R. L. Ray, W. Li & Q. Guo, 2017. Emerging Stress and Relative Resiliency of Giant Sequoia Groves Experiencing Multiyear Dry Periods in a Warming Climate. *Journal of Geophysical Research: Biogeosciences* 122(11):3063-3075 doi:[10.1002/2017JG004005](https://doi.org/10.1002/2017JG004005).
- Sulla-Menashe, D., M. A. Friedl & C. E. Woodcock, 2016. Sources of bias and variability in long-term Landsat time series over Canadian boreal forests. *Remote Sens Environ* 177:206-219 doi:<http://dx.doi.org/10.1016/j.rse.2016.02.041>.
- Tubbesing, C. L., D. L. Fry, G. B. Roller, B. M. Collins, V. A. Fedorova, S. L. Stephens & J. J. Battles, 2019. Strategically placed landscape fuel treatments decrease fire severity and promote recovery in the northern Sierra Nevada. *For Ecol Manage* 436:45-55 doi:<https://doi.org/10.1016/j.foreco.2019.01.010>.
- van Mantgem, P. J., N. L. Stephenson, E. Knapp, J. Battles & J. E. Keeley, 2011. Long-term effects of prescribed fire on mixed conifer forest structure in the Sierra Nevada, California. *For Ecol Manage* 261(6):989-994 doi:<https://doi.org/10.1016/j.foreco.2010.12.013>.
- Varner, J. M., J. M. Kane, J. K. Hiers, J. K. Kreye & J. W. Veldman, 2016. Suites of Fire-Adapted traits of Oaks in the Southeastern USA: Multiple Strategies for Persistence. *Fire Ecology* 12(2):48-64 doi:[10.4996/fireecology.1202048](https://doi.org/10.4996/fireecology.1202048).
- Vernon, M. J., R. L. Sherriff, P. van Mantgem & J. M. Kane, 2018. Thinning, tree-growth, and resistance to multi-year drought in a mixed-conifer forest of northern California. *For Ecol Manage* 422:190-198 doi:<https://doi.org/10.1016/j.foreco.2018.03.043>.
- Walker, R. F., R. M. Fecko, W. B. Frederick, J. D. Murphy, D. W. Johnson & W. W. Miller, 2006. Thinning and Prescribed Fire Effects on Forest Floor Fuels in the East Side Sierra Nevada Pine Type. *Journal of Sustainable Forestry* 23(2):99-115 doi:[10.1300/J091v23n02_06](https://doi.org/10.1300/J091v23n02_06).
- Westerling, A. L., 2016. Increasing western US forest wildfire activity: sensitivity to changes in the timing of spring. *Philosophical Transactions of the Royal Society B: Biological Sciences* 371(1696):20150178 doi:<http://dx.doi.org/10.1098/rstb.2015.0178>.
- Westerling, A. L., H. G. Hidalgo, D. R. Cayan & T. W. Swetnam, 2006. Warming and earlier spring increase western US forest wildfire activity. *science* 313(5789):940-943 doi:[10.1126/science.1128834](https://doi.org/10.1126/science.1128834).
- Whitehead, D. & F. M. Kelliher, 1991. A canopy water balance model for a *Pinus radiata* stand before and after thinning. *Agricultural and Forest Meteorology* 55(1):109-126 doi:[https://doi.org/10.1016/0168-1923\(91\)90025-L](https://doi.org/10.1016/0168-1923(91)90025-L).
- Wittenberg, L., D. Malkinson, O. Beerli, A. Halutzky & N. Tesler, 2007. Spatial and temporal patterns of vegetation recovery following sequences of forest fires in a Mediterranean landscape, Mt. Carmel Israel. *CATENA* 71(1):76-83 doi:<https://doi.org/10.1016/j.catena.2006.10.007>.
- Xiao, J., Q. Zhuang, D. D. Baldocchi, B. E. Law, A. D. Richardson, J. Chen, R. Oren, G. Starr, A. Noormets, S. Ma, S. B. Verma, S. Wharton, S. C. Wofsy, P. V. Bolstad, S. P. Burns, D. R. Cook, P. S. Curtis, B. G. Drake, M. Falk, M. L. Fischer, D. R. Foster, L. Gu, J. L. Hadley, D. Y. Hollinger, G. G. Katul, M. Litvak, T. A. Martin, R. Matamala, S. McNulty, T. P. Meyers, R. K. Monson, J. W. Munger, W. C. Oechel, K. T. Paw U, H. P. Schmid, R. L. Scott, G. Sun, A. E. Suyker & M. S. Torn, 2008. Estimation of net ecosystem carbon exchange for the conterminous United States by combining MODIS and AmeriFlux data. *Agricultural and Forest Meteorology* 148(11):1827-1847 doi:<http://dx.doi.org/10.1016/j.agrformet.2008.06.015>.
- Yang, J., S. Pan, S. Dangal, B. Zhang, S. Wang & H. Tian, 2017. Continental-scale quantification of post-fire vegetation greenness recovery in temperate and boreal North America. *Remote Sens Environ* 199:277-290 doi:<http://dx.doi.org/10.1016/j.rse.2017.07.022>.
- Young, D. J., J. T. Stevens, J. M. Earles, J. Moore, A. Ellis, A. L. Jirka & A. M. Latimer, 2017. Long-term climate and competition explain forest mortality patterns under extreme drought. *Ecol Lett* 20(1):78-86 doi:[10.1111/ele.12711](https://doi.org/10.1111/ele.12711).

Supplementary Material

ET estimation method

We estimated the gridded annual evapotranspiration (ET) from 1985 to 2018 based on the correlations between eddy-covariance flux-tower measurements of annual evapotranspiration and satellite imagery derived NDVI (Equation S1). NDVI was calculated at 30-m resolution from USGS Landsat Collection Tier 1 surface reflectance, downloaded from Google Earth Engine (<https://earthengine.google.com/>). Each annual NDVI map was calculated as the mean of all Landsat scenes for a water year (Oct. to Sept.) after masking for shadow, snow or cloud (Zhu and Woodcock 2012). We homogenized Landsat 8 NDVI (L8, 2014-2018) and Landsat 7 (L7, 2012- 2013) to Landsat 5 NDVI (L5, 1985-2011) following Su et al. (2017); Sulla-Menashe et al. (2016) (Equation S2, S3).

$$ET = 112.3 \times e^{(3.2 \times NDVI)} \quad (S1)$$

$$L5 = 0.9883 \times L7 - 0.0367 \quad (S2)$$

$$L5 = 0.8213 \times L8 - 0.0403 \quad (S3)$$

This Landsat based annual ET estimation was developed by (Goulden et al. 2012; Goulden and Bales 2019), which used 77 site-years of ET data from 10 eddy-covariance flux towers. We extended the estimation with two added flux-tower sites in the study area, resulting in 97 site-years of ET observations, which spanned a wider range of spatial (Fig. 1) and temporal (2001-2016) variations. The 12 flux-towers located in five main vegetation types (Fig. S1). These 12 flux-tower sites also included 4 sites in the Southern California (Fig. 1), which contained representative vegetation types of our study area in the same Mediterranean climate. The ET observations also included some site-years that were impacted by drought, fire, forest thinning, prescribed fire, reflecting by the significant reduction in annual NDVI (Fig. S1). The modeled ET showed a strong correlation to site-level flux-tower observations (coefficient of determination, $R^2=0.77$). Most of the modeled ET fall within ± 100 mm ranges of ET measurements, with a root mean square error (RMSE) at 108 mm, and mean absolute error (MAE) at 74 mm (Figure S1). The main estimation error is observed at site-years with high NDVI and ET values, due to NDVI saturation issue. The model's temporal and spatial sensitivities were assessed using leave-one-out cross validation method by removing an individual water year or flux-tower site for model building and then evaluating on the site-year removed.

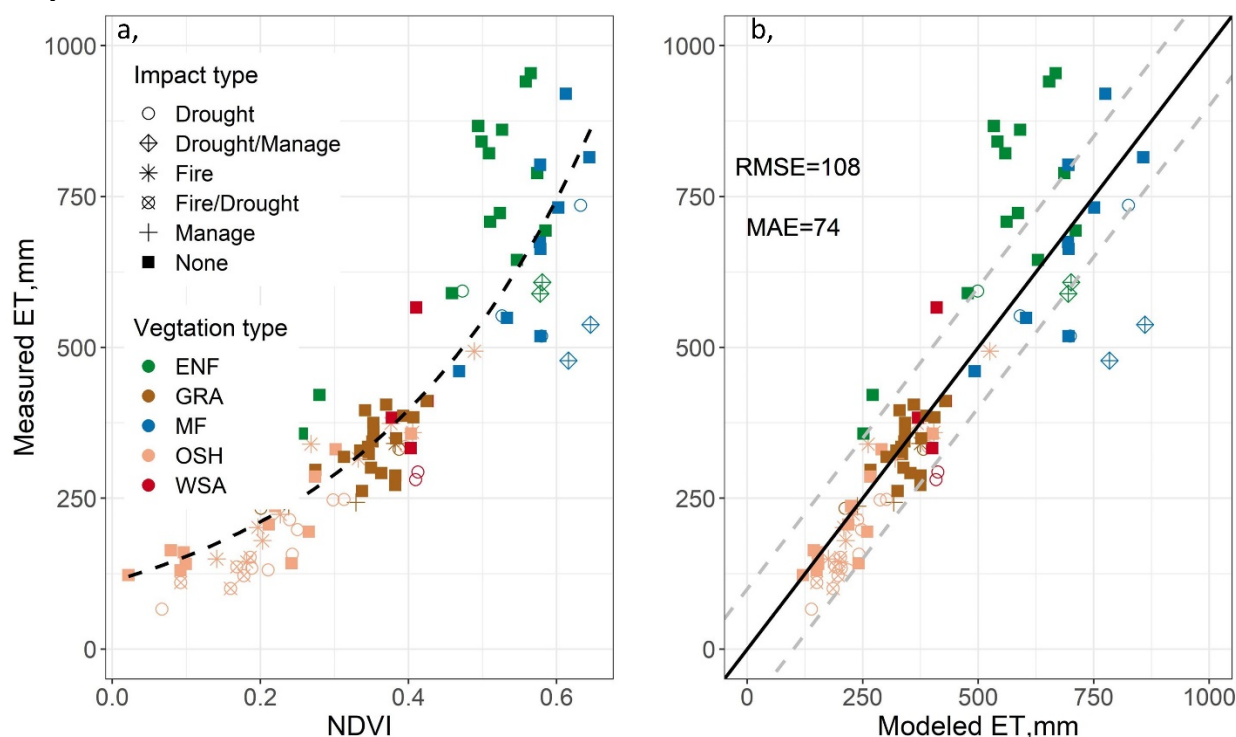


Fig. S1 Flux tower measured annual evapotranspiration (ET) at 97 site-years versus a) annual average Landsat-derived normalized difference vegetation index (NDVI), black dashed line is the exponential fit model (Equation S1); and b) modeled ET, black line is the 1:1 line, and the grey dashed lines are ± 100 mm off the 1:1 line. Root mean square error (RMSE) and mean absolute error (MAE) are given for the model. The color and shape of points indicate vegetation type and impact to vegetation for each site and year. ENF: Evergreen Needleleaf Forest, GRA: Grasslands, MF: Mixed Forest, OSH: Open Shrublands, WSA: Woody Savannas. Manage includes mechanical forest thinning and prescribed fire.

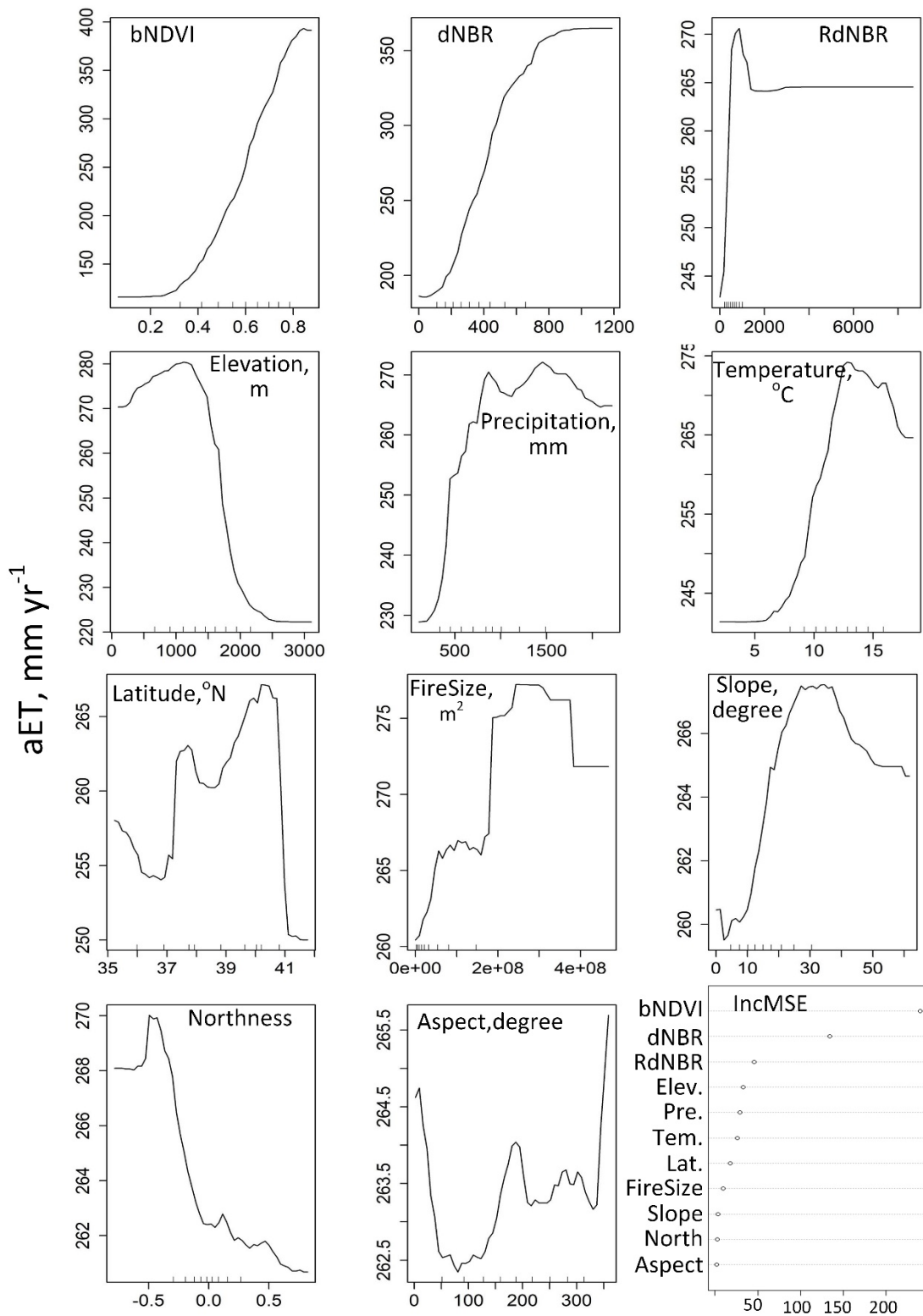


Fig. S3 The random-forest modeled changes in absolute evapotranspiration reduction (aET) across ranges of values for influential variables ordered by the importance: five-year pre-fire NDVI (bNDVI), fire-severity indices dNBR, RdNBR, elevation, precipitation, temperature, latitude, fire size, slope, Northness, and aspect. The importance is calculated from mean decrease accuracy "IncMSE".

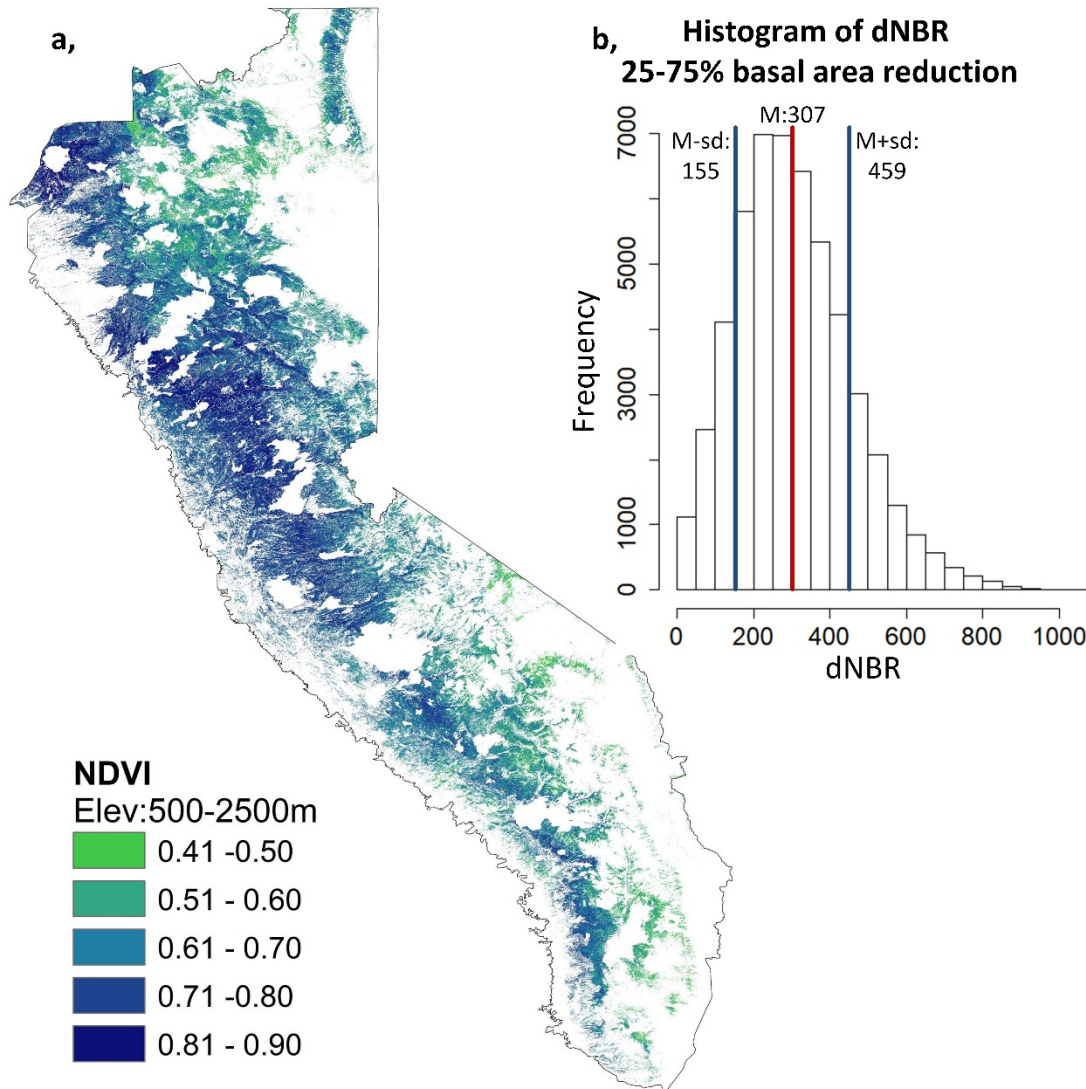


Fig. S4 a) The potential forest area for restoration that haven't been burned by large wildfire in the past 20 years, located in the elevation range of 500-2500-m, with relatively dense vegetation (NDVI>0.4) in the current condition (2018). **b)** The histogram of dNBR values of all the areas burned with 25-75% basal area reduction during 1986-2017. The mean (M) \pm standard deviation (sd) of the dNBR values are label above the histogram, respectively. The current NDVI map and dNBR ranges were used to predict the possible ET reduction.

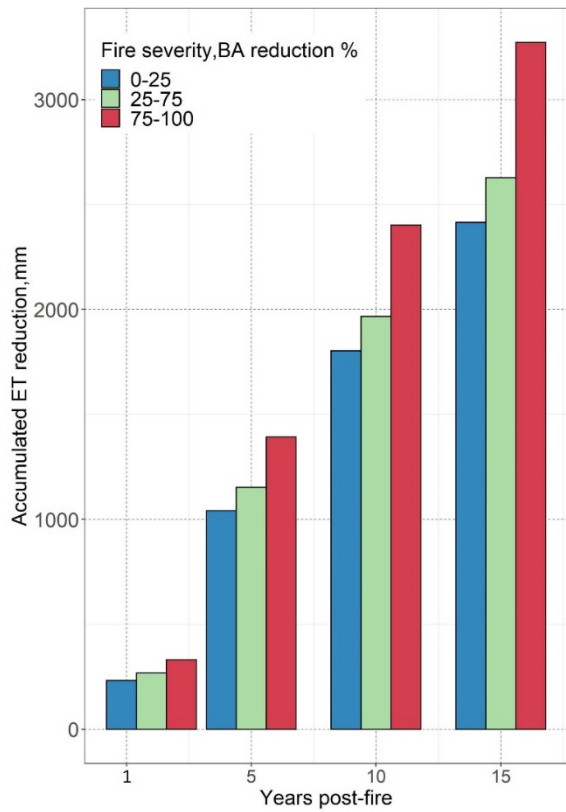


Fig. S5 The accumulated evapotranspiration (ET) reduction to fires of three main severity classes within the first 1, 5, 10, and 15 years following fire, respectively. The values are summarized based on annual mean ET reduction to fires in Fig. 3 in the manuscript.

Table S1 A summary of possible ET reduction for three scenarios over the 1st and 15th year post-fire. The ET reduction in 1st year post-fire with 25-75% basal area reduction (1yrMidSev) was simulated from Equation 4 ($aET=0.41dNBR+622.84bNDVI-234.61$) based on NDVI map with current forest condition and dNBR ranges ($M\pm sd$) from wildfires records (**Fig. S4**). All the other scenarios are calculated based on their ratios (summarized from **Fig. S5**) to the 1yrMidSev.

Scenario			Total ET reduction, bm^3yr^{-1}		
Basal area reduction, %	year post-fire	Ratio to 1yrMidSev.	M-std	M	M+std
25-75	1	1.0	8.7	10.8	13.0
0-25	1	0.9	7.4	9.3	11.1
75-100	1	1.2	10.8	13.5	16.2
0-25	15	0.4	3.5	4.4	5.3
25-75	15	0.5	4.2	5.3	6.3
75-100	15	0.6	5.2	6.5	7.8

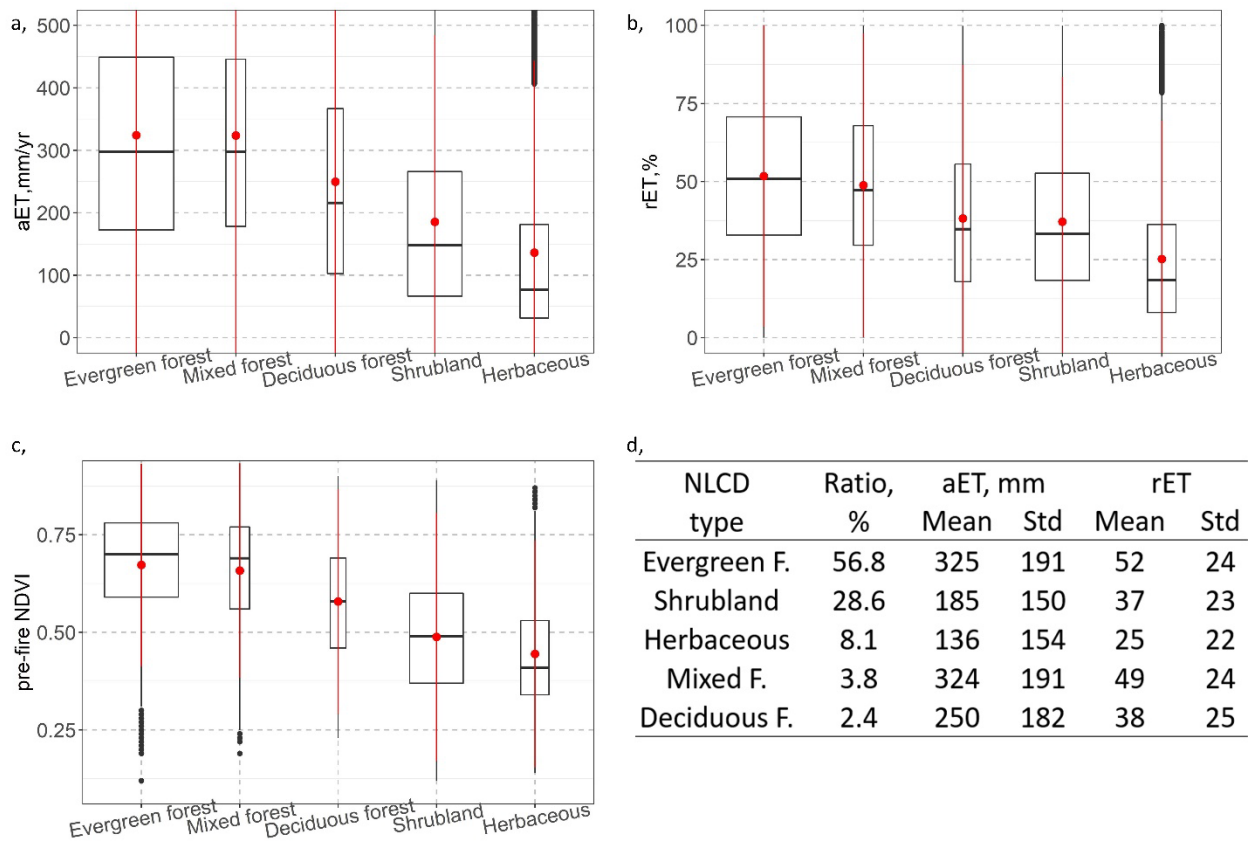
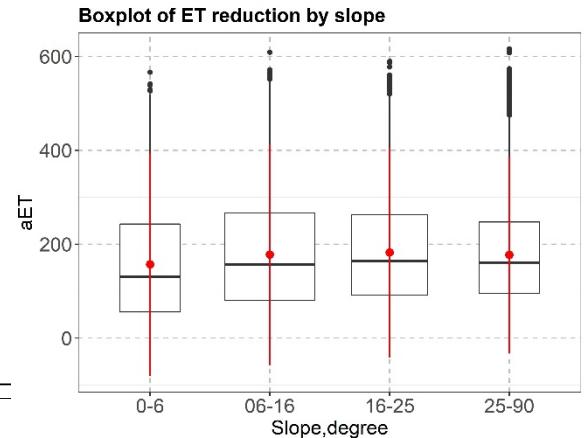
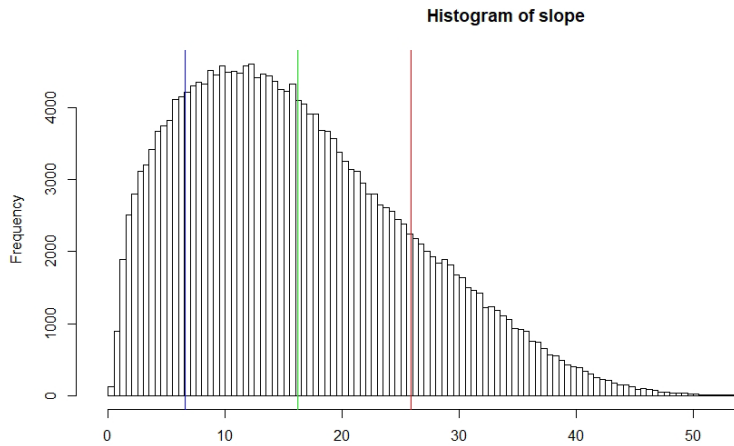


Fig. S6 Boxplots of absolute ET reduction (aET), fractional ET reduction (rET), and pre-fire NDVI in each vegetation types, defined by National Land Cover Database. The red bar indicates the mean and standard deviation of values in each vegetation type. The upper, lower bounds and mid-line of the box indicate the 25%, 75%, and medium values in each vegetation type. The table summarized the portion of burned areas occupied by each vegetation types, and the mean and standard deviation (St) of aET and rET for each vegetation types.

Table S2 The transition of forest type after wildfire. Vegetation type information was obtained from the National Land Cover Database (NLCD 1992, 2001, 2006, 2011, and 2016). The ratio is calculated as the percentage of each forest to other vegetation types.

Pre-fire	Post-fire	Ratio
Deciduous forest	Deciduous forest	66%
	Shrubland	16%
	Herbaceous	15%
	Evergreen forest	3%
Evergreen forest	Evergreen forest	54%
	Herbaceous	25%
	Shrubland	21%
Mixed forest	Mixed forest	46%
	Shrubland	29%
	Herbaceous	12%
	Evergreen forest	10%
	Deciduous forest	2%



Slope groups	aET difference	p value
(16~25) - (0~6)	25.2	0.0
(6~16) - (0~6)	20.9	0.0
(25~90) - (0~6)	20.1	0.0
(16~25) - (25~90)	5.1	0.0
(16~25) - (6~16)	4.3	0.0
(6~16) - (25~90)	0.8	0.6

Slope groups	difference	p value
(16~25) - (25~90)	1%	0
(6~16) - (25~90)	1%	0
(0~6) - (25~90)	1%	0
(6~16) - (16~25)	0%	0.46
(0~6) - (16~25)	0%	0.05
(0~6) - (6~16)	0%	0.47

Northness groups	aET diff	p value
(0.2~0.42)-(-0.02~0.2)	11.3	0.0
(0.2~0.42)-(-0.23~-0.02)	7.1	0.0
(0.2~0.42)-(-0.45~-0.23)	6.9	0.0
(-0.45~-0.23)-(-0.02~0.2)	4.3	0.0
(-0.23~-0.02)-(-0.02~0.2)	4.2	0.0
(-0.45~-0.23)-(-0.23~-0.02)	0.2	1.0

Northness groups	rET diff	p value
(-0.02~0.2)-(-0.45~-0.23)	3%	0.0
(-0.02~0.2)-(-0.23~-0.02)	2%	0.0
(-0.02~0.2)-(0.2~0.42)	1%	0.0
(0.2~0.42)-(-0.45~-0.23)	1%	0.0
(-0.23~-0.02)-(-0.45~-0.23)	1%	0
(0.2~0.42)-(-0.23~-0.02)	0%	0.1

Fig. S7 Difference in aET and rET among Slope and Northness among four groups. The four groups were defined based on the mean (M) and standard deviation (sd) of Slope and Northness ranges, respectively, i.e. Minimum ~ M-sd, M-sd ~ M, M ~ M+sd, M+sd ~ Maxima. Northness is calculated as $Northness = \sin(Slope) \times \cos(Aspect)$.

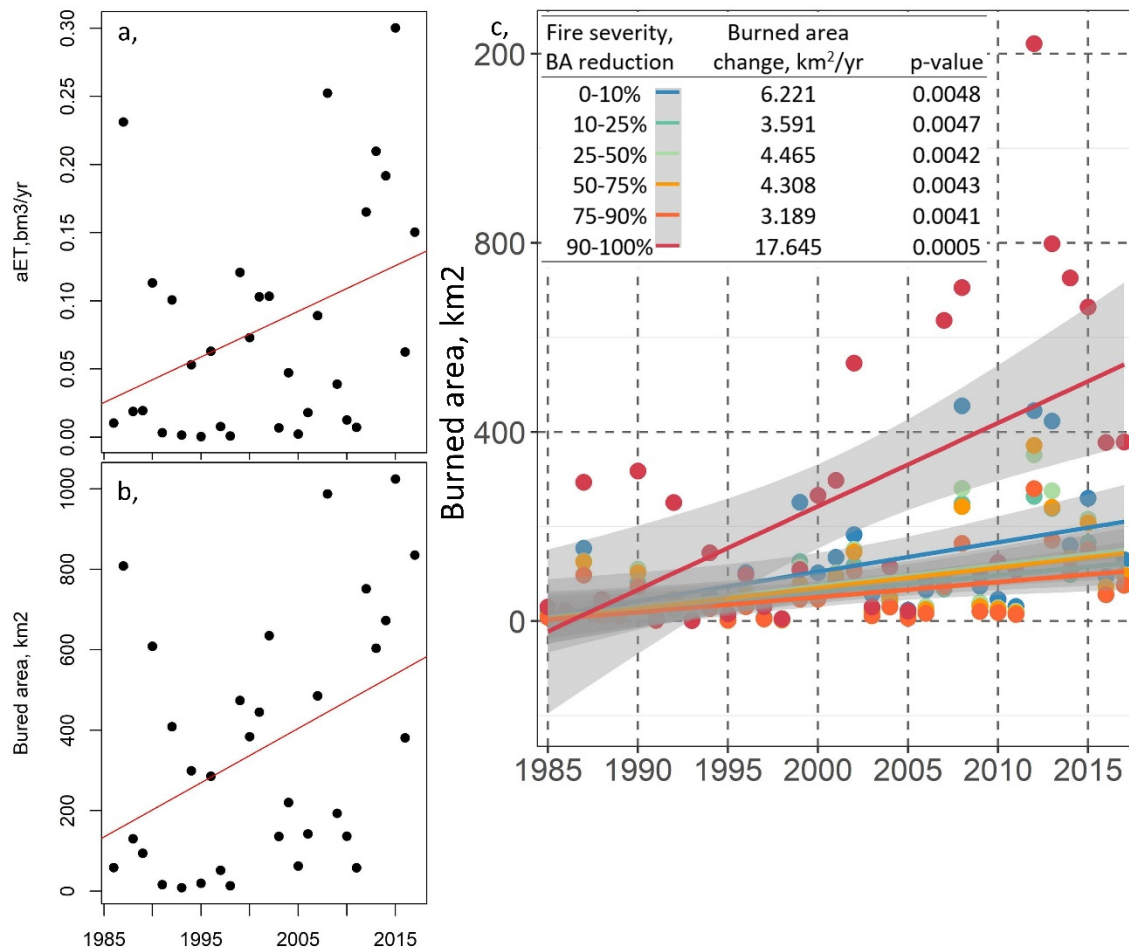


Fig. S8 Time series of total absolute ET reduction (aET, a) and burned area (b) from water year 1986 to 2017. Both variables show increase trend with 0.003 bm^3/year for aET (p value = 0.0344), and 13.5 km^2/year for burned area (p value = 0.0189). Area burned at six fire severity classes is plotted against water year from 1986 to 2017 (c), the class with highest fire severity (90-100% basal area reduction) shows the rapist increase rate over the period (17.6 km^2/year , p value = 0.0005).

References:

- Goulden, M. L., R. G. Anderson, R. C. Bales, A. E. Kelly, M. Meadows & G. C. Winston, 2012. Evapotranspiration along an elevation gradient in California's Sierra Nevada.
- Goulden, M. L. & R. C. Bales, 2019. California forest die-off linked to multi-year deep soil drying in 2012–2015 drought. *Nature Geoscience* doi:10.1038/s41561-019-0388-5.
- Su, Y., R. C. Bales, Q. Ma, K. Nydick, R. L. Ray, W. Li & Q. Guo, 2017. Emerging Stress and Relative Resiliency of Giant Sequoia Groves Experiencing Multiyear Dry Periods in a Warming Climate. *Journal of Geophysical Research: Biogeosciences* 122(11):3063-3075 doi:10.1002/2017JG004005.
- Sulla-Menashe, D., M. A. Friedl & C. E. Woodcock, 2016. Sources of bias and variability in long-term Landsat time series over Canadian boreal forests. *Remote Sens Environ* 177:206-219 doi:<http://dx.doi.org/10.1016/j.rse.2016.02.041>.
- Zhu, Z. & C. E. Woodcock, 2012. Object-based cloud and cloud shadow detection in Landsat imagery. *Remote Sens Environ* 118(Supplement C):83-94 doi:<https://doi.org/10.1016/j.rse.2011.10.028>.